

Malate Plays a Crucial Role in Starch Metabolism, Ripening, and Soluble Solid Content of Tomato Fruit and Affects Postharvest Softening

Danilo C. Centeno,^{a,1} Sonia Osorio,^{a,1} Adriano Nunes-Nesi,^{a,1} Ana L.F. Bertolo,^b Raphael T. Carneiro,^b Wagner L. Araújo,^a Marie-Caroline Steinhauser,^a Justyna Michalska,^a Johannes Rohrmann,^a Peter Geigenberger,^c Sandra N. Oliver,^a Mark Stitt,^a Fernando Carrari,^d Jocelyn K.C. Rose,^b and Alisdair R. Fernie^{a,2}

^a Max-Planck-Institut für Molekulare Pflanzenphysiologie, 14476 Potsdam-Golm, Germany

^b Department of Plant Biology, Cornell University, Ithaca, New York 14853

^c Ludwig-Maximilians-Universität München, Department Biologie I, 82152 Planegg-Martinsried, Germany

^d Instituto de Biotecnología, Centro de Investigación de Ciencias Veterinarias y Agronómicas, Instituto Nacional de Tecnología Agrícola, B1712WAA Castelar, Buenos Aires, Argentina

Despite the fact that the organic acid content of a fruit is regarded as one of its most commercially important quality traits when assessed by the consumer, relatively little is known concerning the physiological importance of organic acid metabolism for the fruit itself. Here, we evaluate the effect of modifying malate metabolism in a fruit-specific manner, by reduction of the activities of either mitochondrial malate dehydrogenase or fumarase, via targeted antisense approaches in tomato (*Solanum lycopersicum*). While these genetic perturbations had relatively little effect on the total fruit yield, they had dramatic consequences for fruit metabolism, as well as unanticipated changes in postharvest shelf life and susceptibility to bacterial infection. Detailed characterization suggested that the rate of ripening was essentially unaltered but that lines containing higher malate were characterized by lower levels of transitory starch and a lower soluble sugars content at harvest, whereas those with lower malate contained higher levels of these carbohydrates. Analysis of the activation state of ADP-glucose pyrophosphorylase revealed that it correlated with the accumulation of transitory starch. Taken together with the altered activation state of the plastidial malate dehydrogenase and the modified pigment biosynthesis of the transgenic lines, these results suggest that the phenotypes are due to an altered cellular redox status. The combined data reveal the importance of malate metabolism in tomato fruit metabolism and development and confirm the importance of transitory starch in the determination of agronomic yield in this species.

INTRODUCTION

The development and maturation of tomato fruits (*Solanum lycopersicum*) has received considerable attention due both to their tractability as a model system and their importance as a component of the human diet (Giovannoni, 2004; Butelli et al., 2008; Matas et al., 2009; Mounet et al., 2009; Wang et al., 2009). Studies of the molecular pathways underlying ripening not only have allowed advances in our understanding of the hormonal and genetic control of the ripening process (Vrebalov et al., 2002; Giovannoni, 2004; Wang et al., 2009) but also have facilitated the targeted genetic engineering of fruit nutritional status and organoleptic characteristics (Römer et al., 2000; Lewinsohn et al., 2001; Dharmapuri et al., 2002; Fraser and Bramley, 2004;

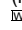
Niggeweg et al., 2004; Davuluri et al., 2005). Despite the fact that there are many studies concerning the genetic and hormonal control of tomato fruit ripening (Barry and Giovannoni, 2006; Cara and Giovannoni, 2008; Seymour et al., 2008) and the temporal regulation of specific areas of ripening related metabolism, such as that of the cell wall (Hadfield and Bennett, 1998; Rose et al., 2004), photosynthetic pigments (Hirschberg, 2001), or phenylpropanoids (Moco et al., 2007), our current understanding of the metabolic shifts that underlie ripening remains somewhat fragmentary (Carrari and Fernie, 2006).

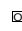
In recent years, a number of postgenomic tools have been applied to the study of tomato fruit ripening, including those targeted at monitoring transcription (Alba et al., 2004; Lemaire-Chamley et al., 2005; Carrari et al., 2006; Vriezen et al., 2008; Wang et al., 2009), translation (Kahlau and Bock, 2008), protein abundance (Saravanan and Rose, 2004; Faurobert et al., 2007), metabolite accumulation (Roessner-Tunali et al., 2003; Carrari et al., 2006; Fraser et al., 2007; Moco et al., 2007), and metabolic flux (Rontein et al., 2002; Tieman et al., 2006). These studies have provided an enormous amount of data, which expands our knowledge of the molecular events associated with ripening, and as such these data are a fertile source for hypothesis generation. However, it is important to note that such studies are somewhat

¹ These authors contributed equally to this work.

² Address correspondence to fernie@mpimpgolm.mpg.de.

The author responsible for distribution of materials integral to the findings presented in this article in accordance with the policy described in the Instructions for Authors (www.plantcell.org) is: Alisdair R. Fernie (fernied@mpimp-golm.mpg.de).

 Online version contains Web-only data.

 Open Access articles can be viewed online without a subscription. www.plantcell.org/cgi/doi/10.1105/tpc.109.072231

restricted with regard to providing direct evidence to support causal mechanisms linking such changes, due in part to the variations in experimental design.

In a previous analysis of metabolic and transcript networks (Carrari et al., 2006), we postulated that three classes of metabolites were particularly important during the ripening process: the cell wall monomers, hexose phosphates, and organic acid intermediates of the tricarboxylic acid (TCA) cycle. Interestingly, as in the previous study, levels of both citrate and malate were also highly correlated to many important regulators of ripening in an independent study that was focused on early fruit development (Mounet et al., 2009). Following these observations, and given that we have a long-standing interest in understanding the role of the TCA cycle in plants (Fernie et al., 2004a; Sweetlove et al., 2007), we decided to first target this pathway. With the exception of two studies (van der Merwe et al., 2009, 2010), our earlier work was focused exclusively on metabolism of the illuminated leaf (Carrari et al., 2003; Nunes-Nesi et al., 2005, 2007; Sienkiewicz-Porzucek et al., 2008). Here, we describe the comprehensive characterization of tomato plants independently exhibiting a fruit-specific decreased expression of genes encoding consecutive enzymes of the TCA cycle: fumarase and malate dehydrogenase (MDH).

Following selection of appropriate genotypes, we demonstrate that targeted changes in the expression of these enzymes in the fruit pericarp result in opposite effects on the total cellular malate content. Interestingly, the rate of starch and pigment synthesis in young fruit and the total soluble solid content of mature fruit, as well as in the postharvest physiology and susceptibility to pathogens, varied between the genotypes. While these phenotypes were not highly correlated to the degree of inhibition of the target enzymes, they closely followed the malate content of the transformants. Detailed biochemical characterization revealed that the changes in starch concentration, and consequently in soluble solids content, were likely due to a redox regulation of ADP-glucose pyrophosphorylase (AGPase). These results are discussed in the context of current theories of the metabolic cues underlying tomato fruit development.

RESULTS

Generation and Screening of Tomato Plants with Fruit-Specific Inhibition of Mitochondrial MDH and Fumarase Activities

An 1860-bp fragment of the cDNA encoding the major tomato fumarase and a 996-bp fragment of the cDNA encoding the only tomato mitochondrial MDH were independently cloned in the antisense orientation between the patatin B33 promoter, which acts as a fruit-specific promoter when expressed in tomato plants (Frommer et al., 1994; Obiadalla-Ali et al., 2004), and the ocs terminator (Figure 1A, i and ii, respectively). Plants obtained by *Agrobacterium tumefaciens*-mediated transformation were grown in the greenhouse, and seeds were collected. Sixteen lines expressing fumarase in antisense and 40 lines expressing the mitochondrial MDH in antisense were selected on the basis of the total cellular activity (see Supplemental Figure 1 online). Six

lines per construct were chosen, which exhibited a range of activities, for further analysis and six T2 plants per line were subsequently grown in the greenhouse. Fruits were harvested at 35 d after flowering (DAF) and assayed for the total activities of fumarase and MDH (Figures 1B and 1C). From these analyses a subset of four lines per construct were selected; F4, F6, F7, and F26 (fumarase) and M14, M21, M23, and M45 (MDH), for detailed biochemical evaluation. To ensure that the reduction of target enzyme activity was restricted to fruits, the activities of the enzymes were additionally tested in both young and mature leaves. In neither instance were the activities altered (see Supplemental Figure 2 online). To confirm that the activities of the target enzymes were reduced on all of the major constituent tissues of the fruit, we dissected fruit from all of the transgenic lines and determined their activities (see Supplemental Figures 3 and 4 online). By contrast to what may have been anticipated from the expression of β -glucuronidase fusion proteins of the B33 promoter, reported by Frommer et al. (2004), our results suggest an approximately equivalent reduction in activity in all tissues.

Malate and Fumarate Levels

Having determined that the transformants displayed the desired alterations in enzyme activities, we next evaluated the levels of the closely associated metabolites, fumarate and malate, using recently developed highly sensitive spectrophotometric assays (Nunes-Nesi et al., 2007). For this purpose, pericarp tissue of green fruit at 35 DAF was harvested and the metabolite content measured. These analyses revealed significant, mild to considerable, decreases in malate and fumarate in all fumarase lines (Figures 1D and 1F). By contrast, the mitochondrial malate dehydrogenase lines were characterized by significant increases in both malate and fumarate levels (Figures 1E and 1G). Relatively consistent changes were also seen in the levels of these metabolites in the other tissues; however, the strongest effect was seen for the pericarp with locular tissues only displaying considerable difference in a subset of the lines (see Supplemental Tables 1 and 2 online).

Fruit Yield

We next determined yield parameters of fully mature fruit. The transformants displayed mild reductions in some lines; however, this was the case for both sets of transformants and moreover was not consistent across the all transgenic lines. Given that total fruit number was essentially unaltered, it appears likely that this was a result of the minor decrease in fruit size exhibited by the lines displaying an altered total fruit weight (significant in lines F6 and F4 [Figure 1H] and M21 [Figure 1I]).

Respiration in Fruits of the Transgenics

As a first experiment, we decided to evaluate the effect of the imposed genetic manipulations on the major pathways of carbohydrate oxidation in the green fruit. For this purpose, we incubated pericarp discs taken from fruits in the light and supplied these with [1- 14 C] or [3,4- 14 C] glucose over a period

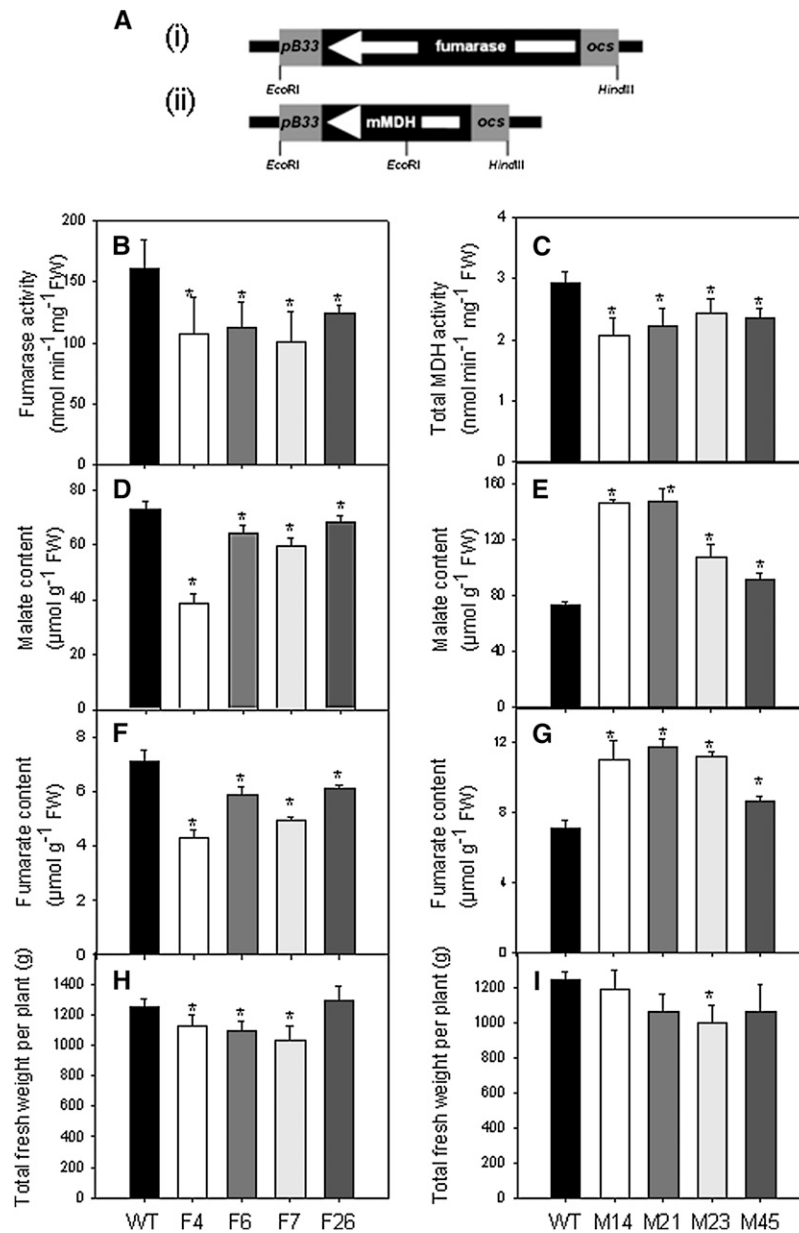


Figure 1. Generation and Preliminary Characterization of Transgenic Lines Expressing Antisense Constructs.

(A) Antisense constructs for tomato mitochondrial fumarase (i) and mitochondrial MDH (ii) under the control of a fruit-specific B33 patatin promoter. White arrows represent the direction of transcription of the native genes. ocs, octopine synthase terminator.

(B) Total fumarase activity in fumarase lines (F4, F6, F7, and F26) relative to the wild type (WT). FW, fresh weight.

(C) Total MDH activity in MDH lines (M14, M21, M23, and M45) relative to the wild type.

(D) and **(E)** Malate content in fumarase **(D)** and MDH **(E)** lines

(F) and **(G)** Fumarate content in fumarase **(F)** and MDH **(G)** lines. The measurements for **(B)** to **(G)** were performed in pericarp of green fruits with 35 DAF.

(H) and **(I)** Total fruit yield of the fumarase **(H)** and MDH **(I)** lines. For all parameters, determined values are presented as the mean \pm SE of 10 biological replicates (total fresh weight per plant is presented as the mean \pm SE of six biological replicates). An asterisk indicates the values that were determined by the *t* test to be significantly different ($P < 0.05$) from the wild type.

of 6 h. During this time, we collected the $^{14}\text{CO}_2$ evolved at hourly intervals. Carbon dioxide can be released from the C1 position by the action of enzymes that are not associated with mitochondrial respiration, but carbon dioxide evolution from the C3:4 positions of Glc cannot (ap Rees and Beevers, 1960). Thus, the ratio of carbon dioxide evolution from C1 to C3:4 positions of Glc provides an indication of the relative rate of the TCA cycle in comparison to other processes of carbohydrate oxidation. The

absolute $^{14}\text{CO}_2$ release from the fumarase lines (Figure 2A), but not the mitochondrial MDH lines, was somewhat elevated (Figure 2B). However, when the relative $^{14}\text{CO}_2$ release of the fumarase and wild-type lines was compared, this was revealed to be unaltered. By contrast, the mitochondrial MDH lines displayed larger changes in their relative rates of $^{14}\text{CO}_2$ release. Both M14 and M23 lines showed a greater relative release of $^{14}\text{CO}_2$ from the C3:4 positions than the wild type, indicating a greater flux through the reactions catalyzed by pyruvate dehydrogenase and malic enzyme.

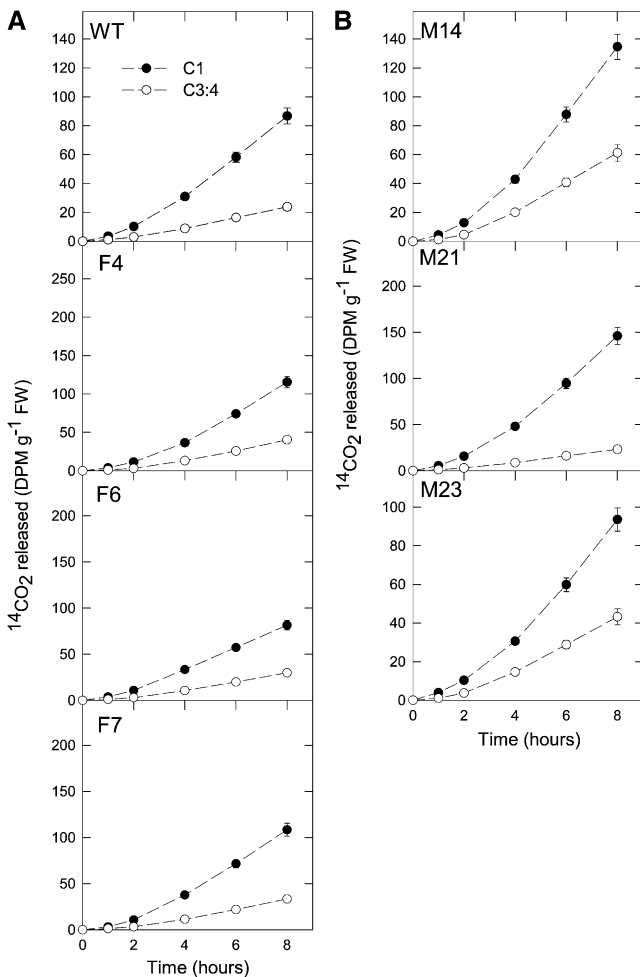


Figure 2. Respiration in Green Fruits of the Antisense Lines Harvested at 35 DAF.

(A) Respiration in mitochondrial fumarase lines. FW, fresh weight; WT, wild type.

(B) Respiration in MDH lines.

Data points show the evolution of $^{14}\text{CO}_2$ from isolated pericarp discs in the light. The pericarp discs were incubated in a solution containing 10 mM MES-KOH, pH 6.5, 0.3 mM Glc, supplemented with 2.32 kBq mL⁻¹ of [1- ^{14}C]- and [3,4- ^{14}C]-glucose at an irradiance of 200 $\mu\text{mol m}^{-2} \text{s}^{-1}$. The $^{14}\text{CO}_2$ liberated was captured (at hourly intervals) in a KOH trap, and the amount of radiolabel released was subsequently quantified by liquid scintillation counting. Values are presented as the mean \pm SE of three biological replicates.

Metabolite Profiles of Green Fruits of the Transformants

Having established that the fruit-specific manipulations of fumarase and the mitochondrial MDH have clear effects on the pericarp levels of malate and fumarate, we next chose to broaden the scope of our metabolite analysis of fruits harvested at 35 DAF using an established gas chromatography–mass spectrometry protocol (Fernie et al., 2004b). Given that this was only one of a large number of comparisons performed, we decided to focus these studies on only two lines per construct. They revealed changes in the levels of a range of sugars, organic acids, and amino acids (see Supplemental Table 5 online).

In the fumarase lines, the levels of several sugars, such as Fru and Glc (lines F4 and F6), maltose (line F6), and Xyl (line F4) decreased significantly (see Supplemental Table 5 online). Similarly, a decrease in the levels of citrate (line F4) and saccharate (both lines) was observed. Intriguingly, the levels of the amino acids β -Ala, Asn, Asp, and Glu were decreased in both lines, while there were unconserved changes in each of the aromatic amino acids and a conserved increase in putrescine (see Supplemental Table 5 online). In the mitochondrial MDH lines, the sugars Fru and Glc also decreased in both lines studied (M14 and M21), with other changes of this compound class being confined to a single line. As would be expected from the spectrophotometric determinations, the organic acids malate and fumarate were increased in these lines, while saccharate again decreased in both lines (see Supplemental Table 5 online). In addition, there was a general decrease in the level of amino acids with conserved decreases in β -Ala, Asn, Asp, Glu, Ile, Lys, Met, Phe, and Trp.

Evaluation of the primary metabolite composition of columela, medulla, and locula tissues of the transformants harvest at the same developmental stage revealed that the pattern of change in metabolites in the first two tissues was highly similar to that observed in the pericarp (compare Supplemental Tables 5 to 7 online). The metabolite profiles of the locular tissue were also largely similar to those of the pericarp; however, for certain metabolites, such as Glc or Asn, the changes in this tissue were quite distinctive (compare Supplemental Tables 5 and 8 online).

Metabolite Profiles of Red-Ripe Fruits of the Transformants

Given that changes in the content of primary metabolites during the ripening process are highly dynamic (Carrari and Fernie, 2006; Carrari et al., 2006; Fraser et al., 2007), we decided also to determine the metabolite content at 65 DAF, a time point that

corresponded to the red-ripe phase of fruit development. In the fumarase lines, similar changes in metabolite content were observed at this developmental stage compared with the wild type, as for the green fruit stage described above. An additional increase in dehydroascorbate was observed for both lines, and by contrast to the situation observed in the green pericarp, the levels of the amino acids Asn, Gln, Gly, Ser, Pro, and Ile increased at this time point (see Supplemental Table 9 online). By contrast, with the exception of displaying decreased levels of Glu, Gly, His, pyroglutamic acid, Glc, and Fru and increased levels of malate, fumarate, Glu, and dehydroascorbate, the MDH lines generally showed less metabolite differences in their pericarp in comparison to that from the wild type than were noted for the green fruit stage.

Evaluation of the primary metabolite composition of columella, medulla, and locula tissues of the transformants harvest at the red-ripe stage revealed that the pattern of change in metabolites was less conserved than at the green stage (compare Supplemental Tables 9 to 12 online). At this time point, with the exception of the generally conserved changes in malate, fumarate, and sugars, most other changes seem to be specific to one or a subset of tissue types.

Sugar and Starch Metabolism in the Transgenics

While gas chromatography–mass spectrometry–based metabolic profiling has proven a very useful tool for plant phenotyping (for details, see Roessner et al., 2001; Fernie et al., 2004b), it does not afford a fully comprehensive coverage of primary metabolism. For this reason, we next profiled the levels of other important metabolites, including sugars, sugar phosphates, adenylates, and uridinylates, inorganic phosphate (Pi), and starch itself, by the use of spectrophotometric or HPLC assays.

The levels of Glc and Fru were significantly lower in the fumarase lines, while Suc was unaltered in green fruit (Table 1). By contrast, in ripe fruit (65 DAF), an increase of up to 40% in sugars was observed to be significant for Glc, Fru (lines F4 and F6), and Suc (line F6). While the MDH lines displayed significant reductions in sugars (Glc, Fru, and Suc) in green fruit, in contrast with the fumarase lines, these metabolites also remained at levels below those observed in the wild type at the red-ripe stage (Table 2).

Decreased levels of hexose phosphate were observed for Glc6P (line F7 and M14), Fru6P (all transgenic lines studied), and Glc1P (lines F4, F7, and F26) in green fruits (Tables 1 and 2). The levels of 3-phosphoglycerate (3PGA), phosphorylated nucleotides, and inorganic phosphate were unaltered in the fumarase-deficient genotypes. By contrast, the mitochondrial MDH-deficient genotypes displayed a significant decrease in 3PGA and in inorganic phosphate as well as decreased levels of ATP and ADP (lines M14, M21, and M45), UTP (line M14), UDP (lines M14 and M21), ADP-glucose (line M14), and UDP-glucose (lines M14, M21, and M45; Table 2). Evaluation of the other major products of the TCA cycle reducing equivalents revealed a decrease in NADPH in green fruits of the mitochondrial MDH but an increase in NAD⁺. Thus, the NADPH/NADP⁺ and NADH/NAD⁺ ratios slightly decreased. The pattern in red fruit is slightly different with NADP⁺ and NAD⁺ decreasing, while the NADPH/

NADP⁺ ratios were unaltered that of NADH/NAD⁺ significantly increases in all lines. A remarkably similar pattern was observed at both developmental stages in the fumarase lines, suggesting that these changes are the consequence of their shared restriction of respiratory activity. Since the adenylate metabolites have previously been demonstrated to be highly important in determining starch content (Regierer et al., 2002; Geigenberger et al., 2005), we next evaluated metabolism of this polymer. As a first experiment, we assessed starch content in green and red fruits of both transgenic sets. Green fruits of the MDH lines displayed substantially lower starch levels (down to 37% of wild-type levels; Table 2), while those of the fumarase lines were dramatically enhanced and even exceeded 250% of the wild-type values (Table 1), with similar although less pronounced changes being apparent in the starch levels of other tissues (see Supplemental Tables 3 and 4 online). As would perhaps be anticipated, the differences in starch content in both transgenic sets were considerably less pronounced in red fruits following degradation of starch and accumulation of carbon in soluble sugars. That said, the changes in starch content in the green fruits of the transgenics were clearly reflected in the above-described changes in sugars, thus confirming starch as an important determinant of soluble solid content at the time of harvest (Baxter et al., 2005).

Given that the transgenic sets exhibited opposite changes in starch content, we next evaluated whether this was a function of total malate content (Figure 3A). A strong negative correlation was seen between malate and starch levels, although this was not entirely linear with even stronger correlations occurring within the independent transgenic sets. However, it was considerably stronger in comparison to the correlation observed between starch and any other metabolite (data not shown).

The regulation of starch synthesis has received much attention in tomato fruit (Beckles et al., 2001) and other heterotrophic organs and tissues (Stark et al., 1992; Tjaden et al., 1998; Jenner et al., 2001; Smidansky et al., 2002; Smith, 2008). A comprehensive metabolic control analysis survey of starch biosynthesis in the potato tuber (*Solanum tuberosum*) revealed that much of the control within this pathway is resident in the import of ATP from the cytosol and in the reaction catalyzed by AGPase (Geigenberger et al., 2004). However, considerable control is also exhibited by enzymes external to the linear pathway of starch synthesis, such as the plastidial adenylate kinase and NAD-dependent malic enzyme. To better understand the alterations in starch metabolism, we next surveyed the activities of a broad range of enzymes of central metabolism (Tables 3 and 4). Activities of these enzymes in the fumarase lines were largely invariant from those observed in the wild type, with the exception of the increase in AGPase activity in the most strongly compromised line, coupled to a decrease in the total cellular MDH activity. In addition, MDH activity was reduced in line F26, while sucrose phosphate synthase (SPS) activity was increased in line F6 (Table 3). Analysis of the MDH lines revealed a significant reduction in AGPase activity (Table 4) as well as those of phosphofruktokinase and shikimate dehydrogenase in line M14 and UDP-glucose pyrophosphorylase (UGPase) in line M45.

Given that previous studies have indicated that the AGPase reaction is redox regulated (Tiessen et al., 2002; Kolbe et al.,

Table 1. Sugar, Phosphorylated Intermediate, and Nucleotide Levels in Both Green and Red Fruit (Harvested 35 and 65 DAF, Respectively) in the Fumarase Lines

Green fruits	Wild Type	F4	F6	F7	F26
Sugars	$\mu\text{mol g}^{-1}$ FW				
Glc	109.63 \pm 5.89	90.04 \pm 3.62	85 \pm 2.43	91.42 \pm 3.68	97.74 \pm 5.24
Fru	104.4 \pm 2.96	91.91 \pm 2.52	88.85 \pm 2.02	94.31 \pm 2.29	96.03 \pm 3.47
Suc	9.31 \pm 0.96	7.57 \pm 0.56	7.27 \pm 0.65	7.4 \pm 0.37	7.54 \pm 0.8
Starch	53.44 \pm 5.25	138.39 \pm 20.87	134.2 \pm 11.81	100.15 \pm 14.15	100.98 \pm 13.31
Sugars-phosphate	nmol g^{-1} FW				
Glc6P	107.94 \pm 10.17	104.05 \pm 3.49	98.25 \pm 7.56	72.54 \pm 2.76	87.08 \pm 9.63
Fru6P	10.51 \pm 1.02	5.76 \pm 0.14	8.37 \pm 1.09	5.37 \pm 0.1	5.3 \pm 0.38
Glc1P	24.39 \pm 3.38	22.27 \pm 1.87	13.93 \pm 0.98	14.41 \pm 1.03	12.17 \pm 0.55
3PGA	45.04 \pm 5.34	47.83 \pm 12.48	40.38 \pm 5.49	55.18 \pm 18.5	65.18 \pm 28.42
Nucleotides	$\mu\text{mol g}^{-1}$ FW				
ATP	22.51 \pm 1.5	26.9 \pm 1.49	26.36 \pm 2.48	26.67 \pm 1.47	20.64 \pm 1.29
ADP	4.27 \pm 0.32	6.3 \pm 0.29	5.07 \pm 0.38	5.76 \pm 0.42	4.58 \pm 0.64
ADP-glucose	1.09 \pm 0.07	1.04 \pm 0.08	1.06 \pm 0.11	0.84 \pm 0.04	0.78 \pm 0.07
UTP	5.72 \pm 0.46	7.31 \pm 0.63	6.68 \pm 0.76	5.02 \pm 0.37	5.54 \pm 0.52
UDP	1.38 \pm 0.23	1.94 \pm 0.25	1.36 \pm 0.16	1.64 \pm 0.25	1.8 \pm 0.39
UDP-glucose	52.77 \pm 1.36	57.35 \pm 2.7	53.35 \pm 1.56	49.17 \pm 2.08	48.84 \pm 4.64
ATP/ADP	5.28 \pm 0.47	4.22 \pm 0.12	5.13 \pm 0.29	4.6 \pm 0.18	2.92 \pm 0.52
UTP/UDP	5.92 \pm 1.2	3.82 \pm 0.42	5.08 \pm 0.75	3.64 \pm 0.9	2.43 \pm 0.67
Pi	1.17 \pm 0.13	1.36 \pm 0.09	1.19 \pm 0.07	0.86 \pm 0.1	0.79 \pm 0.05
3PGA/Pi ratio	44.59 \pm 12.57	36.02 \pm 13.47	32.93 \pm 2.37	62.47 \pm 32.31	49.77 \pm 11.56
Pyridine nucleotide	nmol g^{-1} FW				
NADPH	41.46 \pm 0.83	26.7 \pm 0.69	24.41 \pm 1.48	32.01 \pm 2.28	30 \pm 2.32
NADP	7.74 \pm 0.29	8.93 \pm 0.81	7.21 \pm 0.31	8.54 \pm 1.19	6.98 \pm 0.43
NADP(H)	49.21 \pm 0.55	35.63 \pm 0.72	31.62 \pm 1.52	40.56 \pm 2.15	36.98 \pm 1.9
NADPH/NADP	5.39 \pm 0.3	3.06 \pm 0.29	3.4 \pm 0.25	3.96 \pm 0.59	4.4 \pm 0.56
NADH	60.64 \pm 5.41	65.43 \pm 12.51	88.16 \pm 23.58	63.23 \pm 3.38	56.85 \pm 2.53
NAD	22.14 \pm 1.22	33.06 \pm 4.64	20.49 \pm 2.08	49.12 \pm 8.42	22.05 \pm 1.4
NAD(H)	82.78 \pm 6.61	98.48 \pm 13.5	108.65 \pm 24.89	112.35 \pm 6.66	78.9 \pm 2.99
NADH/NAD	2.73 \pm 0.09	2.12 \pm 0.5	4.2 \pm 0.97	1.52 \pm 0.45	2.61 \pm 0.2
Red fruits	Wild Type	F4	F6	F7	F26
Sugars	nmol g^{-1} FW				
Glc	92.17 \pm 9.08	121.7 \pm 5.62	131.66 \pm 12.59	123.54 \pm 15.27	83.7 \pm 4.12
Fru	101.53 \pm 6.58	124.47 \pm 5.36	135.43 \pm 12.36	128.96 \pm 13.06	94.05 \pm 5.01
Suc	7.05 \pm 0.8	9.3 \pm 1.11	12.18 \pm 2.45	10.04 \pm 2.18	4.32 \pm 0.13
Starch	1.68 \pm 0.14	3.24 \pm 0.49	3.37 \pm 0.36	1.3 \pm 0.03	1.47 \pm 0.02
Nucleotides	$\mu\text{mol g}^{-1}$ FW				
ATP	24.49 \pm 3.62	24.92 \pm 3.82	27.96 \pm 2.84	31.84 \pm 2.44	22.61 \pm 3.59
ADP	7.95 \pm 0.72	7.21 \pm 0.27	7.52 \pm 0.7	8.45 \pm 0.45	6.38 \pm 0.2
ADP-glucose	1.38 \pm 0.1	1.03 \pm 0.08	0.92 \pm 0.05	1.21 \pm 0.14	0.89 \pm 0.14
UTP	11.54 \pm 1.94	9.86 \pm 1.22	9.99 \pm 0.62	14.12 \pm 2.9	10.26 \pm 2.67
UDP	2.04 \pm 0.23	1.73 \pm 0.31	1.46 \pm 0.19	1.81 \pm 0.2	1.21 \pm 0.11
UDP-glucose	69.28 \pm 5.33	45.09 \pm 3.17	44.31 \pm 3.04	55.07 \pm 7.19	47.82 \pm 6.34
ATP/ADP	3.30 \pm 0.4	3.50 \pm 0.49	3.84 \pm 0.16	3.89 \pm 0.27	3.74 \pm 0.8
UTP/UDP	6.20 \pm 0.91	7.66 \pm 2.89	8.69 \pm 3.83	8.26 \pm 1.16	9.04 \pm 3.14
Pyridine nucleotide	nmol g^{-1} FW				
NADPH	52.1 \pm 8.03	65.67 \pm 7.12	37.24 \pm 2.38	65.14 \pm 5.06	69.74 \pm 3.41
NADP	6.15 \pm 1.11	2.58 \pm 0.1	2.19 \pm 0.4	3.71 \pm 0.18	2.85 \pm 0.34
NADP(H)	58.24 \pm 7.16	68.25 \pm 7.16	39.43 \pm 2.35	68.85 \pm 4.93	72.59 \pm 3.41
NADPH/NADP	10.04 \pm 2.97	25.47 \pm 2.58	15 \pm 1.43	17.82 \pm 2.13	25.36 \pm 2.71
NADH	87.43 \pm 7.54	115.72 \pm 11.01	83.63 \pm 7.22	162.58 \pm 9.14	130.86 \pm 9.39
NAD	48.52 \pm 5.35	35.37 \pm 3.55	28.79 \pm 3.09	38.79 \pm 4.16	28.76 \pm 3.13
NAD(H)	135.95 \pm 4.6	151.09 \pm 8.34	112.42 \pm 10.25	201.37 \pm 9.53	159.62 \pm 9.58
NADH/NAD	1.62 \pm 0.18	3.44 \pm 0.57	2.93 \pm 0.10	4.39 \pm 0.65	4.71 \pm 0.63

Values are presented as mean \pm SE of determinations on six individual plants per line (starch in green fruits is presented as the mean \pm SE of 10 biological replicates). Boldface type indicates values that were determined by the *t* test to be significantly different ($P < 0.05$) from the wild type. FW, fresh weight.

Table 2. Sugar, Phosphorylated Intermediate, and Nucleotide Levels in Both Green and Red Fruit (Harvested 35 and 65 DAF, Respectively) in the MDH Lines

Green fruits	Wild Type	M14	M21	M23	M45
Sugars	$\mu\text{mol g}^{-1}$ FW				
Glc	109.63 \pm 5.89	98.91 \pm 0.94	93 \pm 4.25	107.38 \pm 5.67	103.34 \pm 2.43
Fru	104.4 \pm 2.96	91.3 \pm 1.76	82.43 \pm 4.88	100.98 \pm 3.65	95.58 \pm 3.06
Suc	9.31 \pm 0.96	7.32 \pm 0.41	7.41 \pm 0.36	8.65 \pm 1.22	7.04 \pm 0.42
Starch	53.44 \pm 5.25	19.85 \pm 5.03	24.46 \pm 11.49	25.15 \pm 9.93	44.86 \pm 10.11
Sugars-phosphate	nmol g^{-1} FW				
Glc6P	107.94 \pm 10.17	74.12 \pm 5.19	87.46 \pm 6.87	93.52 \pm 8.47	90.18 \pm 7.03
Fru6P	10.51 \pm 1.02	8.89 \pm 0.35	8.04 \pm 0.28	9.11 \pm 0.22	8.04 \pm 0.2
Glc1P	24.39 \pm 3.38	18.58 \pm 4.4	19.09 \pm 4.05	31.64 \pm 4.79	27.46 \pm 8.22
3PGA	45.04 \pm 5.34	35.15 \pm 6.36	39.85 \pm 10.51	22.98 \pm 3.5	40.38 \pm 7.08
Nucleotides	nmol g^{-1} FW				
ATP	22.51 \pm 1.5	12.86 \pm 0.66	15.53 \pm 1.05	22 \pm 0.78	14.62 \pm 1.39
ADP	4.27 \pm 0.32	1.12 \pm 0.04	1.54 \pm 0.09	3.41 \pm 0.43	2.91 \pm 0.2
ADP-glucose	1.09 \pm 0.07	0.83 \pm 0.05	0.99 \pm 0.04	1.11 \pm 0.05	0.95 \pm 0.05
UTP	5.72 \pm 0.46	3.00 \pm 0.22	5.62 \pm 1.74	6.69 \pm 0.59	4.72 \pm 1.38
UDP	1.38 \pm 0.23	1.05 \pm 0.02	1.11 \pm 0.04	1.33 \pm 0.07	1.40 \pm 0.08
UDP-glucose	52.77 \pm 1.36	37.06 \pm 1.41	43.59 \pm 1.11	47.5 \pm 2.54	42.51 \pm 2.13
ATP/ADP	5.28 \pm 0.47	12.5 \pm 6.93	10.46 \pm 1.82	7.18 \pm 2.61	5.13 \pm 0.58
UTP/UDP	5.92 \pm 1.2	4.08 \pm 0.19	7.02 \pm 1.21	7.19 \pm 0.22	4.78 \pm 0.34
Pi	1.17 \pm 0.13	0.78 \pm 0.05	1 \pm 0.11	1.05 \pm 0.1	0.94 \pm 0.02
3PGA/Pi ratio	44.59 \pm 12.57	57.41 \pm 13.64	50.41 \pm 12.51	24.82 \pm 2.4	52.59 \pm 8.51
Pyridine nucleotide	nmol g^{-1} FW				
NADPH	41.46 \pm 0.83	32.29 \pm 2	31.7 \pm 0.49	29.19 \pm 1.06	31.79 \pm 3.27
NADP	7.74 \pm 0.29	6.47 \pm 0.24	8.17 \pm 0.3	7.82 \pm 0.26	7.16 \pm 0.49
NADP(H)	49.21 \pm 0.55	38.77 \pm 2.2	39.87 \pm 0.78	37.01 \pm 1.22	38.95 \pm 3.59
NADPH/NADP	5.39 \pm 0.3	4.98 \pm 0.19	3.89 \pm 0.08	3.74 \pm 0.12	4.44 \pm 0.37
NADH	60.64 \pm 5.41	58.34 \pm 3.63	56.01 \pm 1.46	60.82 \pm 2.32	58.92 \pm 3.04
NAD	22.14 \pm 1.22	19.34 \pm 1.56	35.35 \pm 7.84	37.78 \pm 2.38	22.41 \pm 0.77
NAD(H)	82.78 \pm 6.61	77.69 \pm 4.72	91.36 \pm 8.18	98.6 \pm 1.6	81.32 \pm 2.49
NADH/NAD	2.73 \pm 0.09	3.06 \pm 0.23	1.86 \pm 0.46	1.64 \pm 0.17	2.65 \pm 0.22
Red fruits	Wild Type	M14	M21	M23	M45
Sugars	$\mu\text{mol g}^{-1}$ FW				
Glc	92.17 \pm 9.08	79.49 \pm 6.01	72.11 \pm 6.25	84.13 \pm 4.39	78.68 \pm 1.53
Fru	101.53 \pm 6.58	89.85 \pm 5.84	83.7 \pm 6.28	97.41 \pm 3.03	96.36 \pm 1.01
Suc	7.05 \pm 0.8	4.95 \pm 0.32	4.55 \pm 0.32	5.57 \pm 0.25	5.07 \pm 0.14
Starch	1.57 \pm 0.14	1.25 \pm 0.35	1.15 \pm 0.46	1.24 \pm 0.39	2.19 \pm 1.45
Nucleotides	$\mu\text{mol g}^{-1}$ FW				
ATP	24.49 \pm 3.62	23.56 \pm 3.91	26.26 \pm 2.85	23.83 \pm 1.34	26.31 \pm 3.47
ADP	7.95 \pm 0.72	7.49 \pm 0.27	7.5 \pm 0.25	8.12 \pm 0.45	6.65 \pm 0.31
ADP-glucose	1.38 \pm 0.1	1.54 \pm 0.19	1.14 \pm 0.12	1.35 \pm 0.23	0.97 \pm 0.08
UTP	11.54 \pm 1.94	11.34 \pm 1.17	13.22 \pm 2.53	7.93 \pm 0.63	10.14 \pm 1.72
UDP	2.04 \pm 0.23	1.79 \pm 0.29	1.44 \pm 0.1	1.23 \pm 0.13	1.08 \pm 0.15
UDP-glucose	69.28 \pm 5.33	70.93 \pm 8.38	55.76 \pm 7.45	49.05 \pm 4.17	47.49 \pm 3.94
ATP/ADP	3.3 \pm 0.4	3.57 \pm 0.65	3.77 \pm 0.35	2.9 \pm 0.19	3.81 \pm 0.32
UTP/UDP	6.2 \pm 0.91	8.96 \pm 1.24	11.84 \pm 1.98	7.61 \pm 0.57	10.11 \pm 1.21
Pyridine nucleotide	nmol g^{-1} FW				
NADPH	52.1 \pm 8.03	56.18 \pm 6.88	51.45 \pm 5.09	45.07 \pm 2.59	47.26 \pm 2.31
NADP	6.15 \pm 1.11	3.56 \pm 0.47	2.84 \pm 0.28	2.55 \pm 0.39	4.25 \pm 0.37
NADP(H)	58.24 \pm 7.16	59.74 \pm 6.53	54.29 \pm 4.91	47.62 \pm 2.2	51.51 \pm 2.59
NADPH/NADP	10.04 \pm 2.97	12.97 \pm 1.25	19.06 \pm 3.35	19.38 \pm 3.77	11.31 \pm 0.78
NADH	87.43 \pm 7.54	100.77 \pm 19.55	128.81 \pm 10.3	87.22 \pm 4.38	103.18 \pm 4.33
NAD	48.52 \pm 5.35	28.46 \pm 1.98	27.17 \pm 2.82	27.74 \pm 1.88	30.32 \pm 3.44
NAD(H)	135.95 \pm 4.6	111.33 \pm 6.91	155.98 \pm 9.64	114.96 \pm 6.03	133.5 \pm 5.92
NADH/NAD	1.62 \pm 0.18	3.63 \pm 0.75	4.99 \pm 0.91	3.16 \pm 0.12	3.54 \pm 0.45

Values are presented as mean \pm SE of determinations on six individual plants per line (starch in green fruits is presented as the mean \pm SE of 10 biological replicates). Boldface type indicates values that were determined by the *t* test to be significantly different ($P < 0.05$) from the wild type. FW, fresh weight.

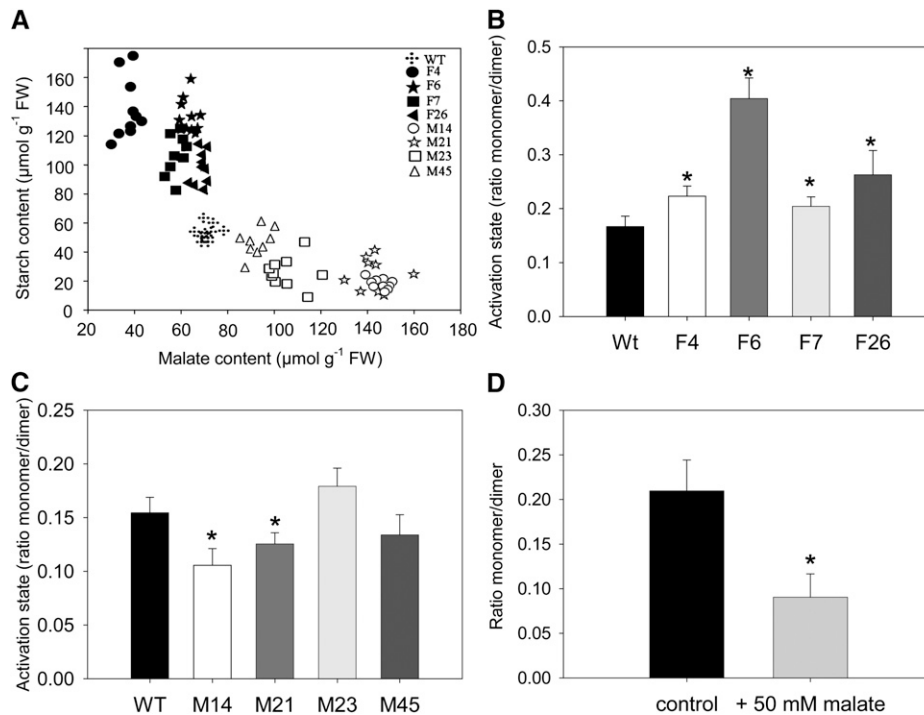


Figure 3. Starch Metabolism in Pericarp Discs from Green Fruits Harvested at 35 DAF in the Antisense Fumarase and MDH Lines.

(A) Regression analysis of malate and starch content in all genotypes studied: $R_F = 0.608$, $R_M = 0.744$, $R_{F+M} = 0.841$. Crosses, wild-type (WT/Wt) lines; closed symbols, fumarase lines; open symbols, MDH lines; FW, fresh weight.

(B) and **(C)** Analysis of the dimerization of AGPase in fumarase **(B)** and MDH **(C)** lines.

(D) Evaluation of the dimerization of AGPase following incubation of wild-type pericarp discs in 50 mM malate.

Values in **(B)** to **(D)** are presented as mean \pm SE of determinations on 10 individual plants per line. Asterisks indicate values that were determined by the *t* test to be significantly different ($P < 0.05$) from the wild type.

2005), we next evaluated the activation states of both the AGPase reaction and that of the plastidic MDH. The activation state of the latter has previously been demonstrated to be a reliable marker for alteration of the plastidial redox environment (Foyer et al., 1992; Scheibe, 1991). A clear tendency of an increased activation state of NADP-MDH was observed in the fumarase lines; this being statistically significant in the lines F4 and F6 (and a similar order of magnitude in the other lines; Table 3). Conversely, in the MDH lines, the activation state showed a clear trend of decreasing and was significantly so in lines M21 and M14 (Table 4).

It has been demonstrated that AGPase is redox regulated, being more active in the monomeric state (Fu et al., 1998; Tiessen et al., 2002). To investigate the activation status of AGPase, we evaluated the ratio of monomerization to dimerization of the protein via separation on nonreducing SDS gels. An increasing level of dimerization of AGPaseB (AGPB) has previously been demonstrated to lead to a greater inactivation of the protein as a result of a marked decrease of the substrate affinity and sensitivity to allosteric effectors (Iglesias et al., 1993; Ballicora et al., 1995; Tiessen et al., 2002). We observed that green fruits of the fumarase lines exhibited a greater proportion of AGPB in the monomerized state than the wild type (significantly so in all lines; Figure 3B), while the MDH lines tended toward a reduced ratio of

monomerized:dimerized AGPB (significantly so in line M14 and M21; Figure 3C). Intriguingly, the changes in the proportion of AGPase in the monomerized state matched the changes in starch content, which was also increased in fumarase lines and decreased in MDH lines.

To better understand these observations, we performed two further experiments. First, we analyzed the activity of the AGPase enzyme under reducing and nonreducing conditions. Second, we evaluated the expression of genes encoding the small and large subunits of the AGPase. To carry out the first experiment, we assayed enzyme extracts in presence (reducing) or absence (oxidizing) 4 mM DTT; furthermore, this reductant was either added to the incubation buffer or not, according to Tiessen et al. (2002). Three of the fumarase lines (F7, F4, and F6) displayed an increased AGPase activity, whereas two of the MDH lines (M21 and M14) displayed decreased AGPase activity. By contrast, only one of the fumarase lines (F7) displayed an increased AGPase activity in the fumarase lines, whereas all of the MDH lines exhibited a decrease in AGPase activity under these assay conditions.

In a complementary experiment, we evaluated the expression levels of the small subunit and large subunit 1 and 2 genes of the transgenics in samples taken at around the breaker stage. The fumarase lines exhibited minor changes

Table 3. Enzymatic Activities in Both Green and Red Fruit (Harvested 35 and 65 DAF, Respectively) in the Fumarase Lines

Enzymatic Activities	Wild Type	F4	F6	F7	F26
Green fruits	nmol min ⁻¹ g ⁻¹ FW				
Phosphofructokinase	79.13 ± 9.25	88.27 ± 10.32	76.43 ± 8.93	80.51 ± 9.41	75.84 ± 8.86
Pyruvate kinase	82.68 ± 21.21	57.06 ± 14.64	70.48 ± 18.08	107.58 ± 27.60	112.57 ± 28.87
AGPase (+PGA)	10.48 ± 1.03	14.56 ± 0.85	14.55 ± 1.18	14.11 ± 1.07	10.56 ± 1.49
AGPase (-PGA)	8.63 ± 0.78	15.94 ± 1.38	11.51 ± 0.92	9.55 ± 1.06	10.32 ± 0.95
Shikimate DH	21.52 ± 0.99	21.14 ± 0.97	23.83 ± 1.10	21.22 ± 0.98	23.73 ± 1.09
UGPase	92.52 ± 4.58	89.60 ± 4.43	88.48 ± 4.38	88.47 ± 4.38	76.21 ± 3.77
SPS	178.68 ± 16.83	161.06 ± 15.17	138.99 ± 13.09	181.68 ± 17.12	139.41 ± 13.13
Succinyl CoA ligase	165.53 ± 43.20	172.75 ± 45.09	191.30 ± 49.93	168.40 ± 43.95	159.17 ± 41.54
NAD-MDH	3516.70 ± 258.40	3313.70 ± 243.50	3226.70 ± 237.10	3394.60 ± 249.40	2674.30 ± 196.50
NADP-MDH initial	0.09 ± 0.02	0.12 ± 0.01	0.11 ± 0.01	0.10 ± 0.01	0.07 ± 0.01
NADP-MDH total	0.30 ± 0.02	0.28 ± 0.00	0.24 ± 0.03	0.23 ± 0.02	0.19 ± 0.03
NADP-MDH activation state	0.31 ± 0.04	0.45 ± 0.02	0.49 ± 0.03	0.45 ± 0.06	0.41 ± 0.07
Red fruits	nmol min ⁻¹ g ⁻¹ FW				
Phosphofructokinase	51.68 ± 4.96	53.88 ± 5.17	55.78 ± 5.36	46.32 ± 4.45	57.21 ± 5.49
Pyruvate kinase	79.06 ± 24.71	78.69 ± 24.60	71.53 ± 22.36	50.31 ± 15.73	78.22 ± 24.45
AGPase	3.16 ± 1.04	2.60 ± 0.85	3.72 ± 1.22	4.07 ± 1.34	2.20 ± 0.72
Shikimate DH	22.54 ± 3.58	20.47 ± 3.25	23.89 ± 3.79	23.14 ± 3.67	22.77 ± 3.61
UGPase	55.49 ± 5.58	60.75 ± 6.11	64.53 ± 6.49	68.30 ± 6.87	44.06 ± 4.43
SPS	125.34 ± 8.36	129.68 ± 8.65	146.00 ± 9.73	149.12 ± 9.94	126.77 ± 8.45

Values are presented as mean ± SE of determinations on six individual plants per line. Boldface type indicates values that were determined by the *t* test to be significantly different ($P < 0.05$) from the wild type. FW, fresh weight.

in expression of the small subunit around breaker, and the expression of the large subunit 1 was more highly expressed in four and three of these lines at breaker-3 and breaker-1, respectively. By contrast, the MDH lines exhibited only a minor decrease in expression of the large subunit 1 at breaker-3 (Figure 4). When taken together, these combined data, alongside that of the plastidial MDH, support an altered plastidial redox status. This suggests that despite their similar overall levels, the pyrimidine nucleotides are likely to display differential subcellular location in the different transgenic sets. Unfortunately, we were not able to confirm this fact given the technical difficulty of performing such measurements in tomato fruit (data not shown).

Metabolic Fluxes in the Transgenics

We next assessed the major fluxes of carbon metabolism in two lines of each transgenic set and in the wild type by incubating excised pericarp discs from green fruit in a buffer containing 10 mM [¹⁴C]glucose (specific activity 1.4 MBq mmol⁻¹) for a period of 2 h. Following this incubation, the discs were thoroughly washed, snap-frozen in liquid nitrogen, and fractionated on the basis of chemical composition as described by Carrari et al. (2006). Consistent with the results of previous studies (Rontein et al., 2002; Carrari et al., 2006), the tissue was highly metabolically active, with the dominant flux being that of Suc synthesis. The fumarase lines were characterized by relatively similar rates of uptake and radiolabel distribution to those observed in the wild type. The only notable exception was that the rates of label redistribution to Suc and Fru synthesis were significantly decreased. However, when the absolute fluxes, which also account for radiolabel dilution (Geigenberger et al.,

2000), were taken into account, a clear increase could be seen in the flux to starch (Table 5). The increased rate of starch synthesis was coupled to a decrease in the rate of Suc synthesis and, at least in the case of line F4, of glycolysis. As evidenced by the starch:Suc and starch:glycolysis ratios, these data clearly suggest a strong metabolic shift in favor of starch synthesis within these lines. The MDH lines exhibited no significant changes in the uptake of radiolabel; however, line M14 displayed significantly lower redistribution of radiolabel to phosphate esters, organic acids, and Suc. In contrast with the fumarase lines, however, these lines displayed relatively little changes in absolute fluxes, with the flux to starch in line M14 and the ratio of starch and Suc biosynthesis in both lines being the only parameters that were significantly different from wild-type values.

Metabolic Fluxes after Incubation in Malate

Given that elevating the cellular malate content resulted in alteration in the properties of AGPase in the transgenic plants, we next tested its effect on the flux to starch by incubation of pericarp discs in buffer containing malate. For this purpose, we incubated pericarp discs in varying concentrations of malate (0 to 70 mM) for a period of 2 h in addition to 10 mM [¹⁴C] glucose (specific activity 1.5 MBq mmol⁻¹). Interestingly, the presence of malate in the medium resulted in a concentration-dependent decrease in the rates of Glc uptake (Table 6). The reduced glucose uptake rate did not cause any alteration of radiolabel distribution in the soluble fraction comprising organic acids, amino acids, Suc, and Fru. However, when the insoluble fractions were analyzed, a strong malate concentration-dependent reduction in the proportional incorporation of label in starch was observed.

Table 4. Enzymatic Activities in Both Green and Red Fruit (Harvested 35 and 65 DAF, Respectively) in the MDH Lines

Enzymatic Activities	Wild Type	M14	M21	M23	M45
Green fruits	nmol min ⁻¹ g ⁻¹ FW				
Phosphofructokinase	79.13 ± 9.25	52.8 ± 6.17	77.58 ± 9.07	70.31 ± 8.22	79.85 ± 9.33
Pyruvate kinase	82.68 ± 21.21	80.16 ± 20.56	66.26 ± 17	110.89 ± 28.44	109.96 ± 28.21
AGPase (+PGA)	10.48 ± 1.03	6.6 ± 0.6	7.74 ± 0.34	7.89 ± 0.46	8.25 ± 0.47
AGPase (-PGA)	8.63 ± 0.78	5.77 ± 0.76	6.28 ± 0.21	5.55 ± 0.69	6.52 ± 0.48
Shikimate DH	21.52 ± 0.99	15.09 ± 0.7	21.44 ± 0.99	27.38 ± 1.26	22.79 ± 1.05
UGPase	92.52 ± 4.58	90.02 ± 4.45	95.66 ± 4.73	84.57 ± 4.18	96.95 ± 4.8
SPS	178.68 ± 16.83	153.39 ± 14.45	197.7 ± 18.62	155.43 ± 14.64	179.47 ± 16.91
Succinyl CoA ligase	165.53 ± 43.2	159.99 ± 41.76	160.32 ± 41.85	173.03 ± 45.16	136.55 ± 35.64
Fumarase	194.02 ± 49.63	354.1 ± 90.58	268.16 ± 68.6	336.61 ± 86.11	0 ± 0
NADP-MDH initial	0.1 ± 0.01	0.08 ± 0.01	0.09 ± 0.01	0.08 ± 0.01	0.08 ± 0.01
NADP-MDH total	0.26 ± 0.01	0.19 ± 0.01	0.23 ± 0.01	0.21 ± 0.02	0.22 ± 0.02
NADP-MDH activation state	0.41 ± 0.01	0.36 ± 0.01	0.36 ± 0.01	0.38 ± 0.01	0.39 ± 0.03
Red fruits	nmol min ⁻¹ g ⁻¹ FW				
Phosphofructokinase	51.68 ± 4.96	52.73 ± 5.06	48.59 ± 4.67	65.6 ± 6.3	44.87 ± 4.31
Pyruvate kinase	79.06 ± 24.71	64.15 ± 20.05	117.3 ± 36.67	64.64 ± 20.21	92.92 ± 29.05
AGPase	3.16 ± 1.04	3.25 ± 1.07	3.47 ± 1.14	2.42 ± 0.8	1.68 ± 0.55
Shikimate DH	22.54 ± 3.58	21.18 ± 3.36	20.14 ± 3.2	22.69 ± 3.6	18.59 ± 2.95
UGPase	55.49 ± 5.58	51.05 ± 5.13	43.3 ± 4.35	62.71 ± 6.3	37.98 ± 3.82
SPS	125.34 ± 8.36	114.96 ± 7.66	120.91 ± 8.06	134.23 ± 8.95	86.45 ± 5.76

Values are presented as mean ± SE of determinations on six individual plants per line. Boldface type indicates values that were determined by the *t* test to be significantly different (*P* < 0.05) from the wild type. FW, fresh weight.

Because interpretation of the distribution of radiolabel can be complicated by differential mobilization of internal, unlabeled storage reserves (Geigenberger et al., 1997, 2000), we next measured the levels of phosphate esters in these samples. Following these measurements, we determined that the specific activity of this pool, in the presence different concentrations of malate, was unaltered. Estimation of the absolute fluxes revealed a concentration-dependent reduction in the rates of starch biosynthesis, which was coupled with a considerable reduction in the flux to Suc. When taken together, these results suggest that changes in malate content influence the activation state of AGPase and, thus, the rate of starch synthesis. To validate this hypothesis, we incubated excised pericarp discs from green wild-type fruit in a buffered solution in the presence or absence of 50 mM malate and analyzed the dimerization (activation) state of AGPase. As predicted, assuming malate has an influence on the AGPase, the samples incubated in malate displayed a significant reduction in the ratio of monomerized to dimerized AGPase in the malate-fed samples, substantiating our hypothesis (Figure 3D), whereas samples incubated in 50 mM mannitol as an osmotic control had no discernable effect on this parameter (see Supplemental Figure 5 online).

Pigment Levels

Changes in fruit color are among the most obvious visual characteristics defining processes occurring during fruit ontogeny (Pecker et al., 1992). Overall color change is the result of differential pigment accumulation; so to use this as a means to monitor potential effects of the two transgenes on fruit development, we evaluated the levels of the pigments chlorophyll *a* and *b*, β-carotene, lutein, neoxanthin, violaxanthin, zeaxanthin, an-

theraxanthin, and lycopene in fruits harvested between 20 and 65 DAF (see Supplemental Tables 18 and 19 online). The pigment profile of the wild-type plants was in accordance with previous reports (Fraser et al., 1994; Bramley, 2002; Carrari et al., 2006), with progressive declines in the levels of the chlorophylls, antheraxanthin, neoxanthin, and violaxanthin and increases in the levels of β-carotene and, most dramatically, lycopene. The levels of pigments in the transgenics were very similar at 20 DAF; however, by 35 DAF, clear differences were apparent, with decreases in β-carotene, the chlorophylls, lutein, and violaxanthin in the MDH lines and a tendency for these compounds (with the exception of violaxanthin) to increase in the fumarase lines. At 48 DAF, the chlorophyll *a* content was significantly reduced in lines M23 and M21, but also in line F4. By contrast, at 56 DAF, the level of chlorophyll *a* was up to fourfold higher in the MDH line M23 but marginally lower in the fumarase lines. At 60 DAF, the clearest difference between the genotypes was that the levels of lycopene were significantly higher in the MDH plants (all lines) but marginally reduced in the fumarase line F6.

To complement the above study, we decided to perform a range of metabolite profiling experiments shortly before (−3 and −1 d), during (+3 and +1 days), and after breaking using the exact same material as that harvested for the quantitative RT-PCR (qRT-PCR) experiments described in Figure 4. These studies revealed a large amount of metabolic variance during these time points; however, it is notable that changes in metabolite levels are often not conserved across the independent lines of a transgenic set or even are varying in opposing directions (see Supplemental Tables 13 to 17 online). Moreover, when the relative levels of metabolites are surveyed across the entire data set, no systematic delay or acceleration in the patterns of metabolic change becomes apparent (data not shown).

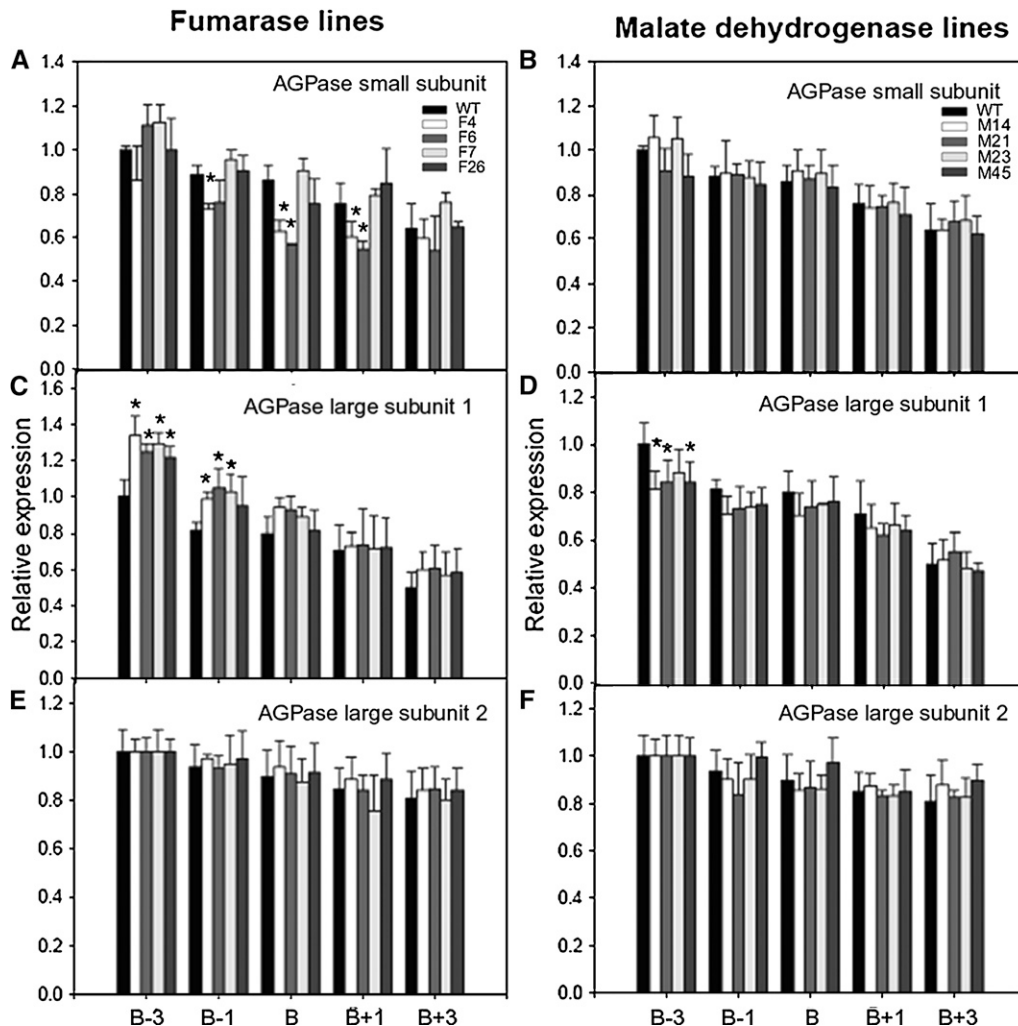


Figure 4. Gene Expression of AGPase Small Subunit and AGPase Large Subunit 1 and 2 in Antisense Lines.

(A) and (B) AGPase small subunit expression in fumarase (A) and MDH (B) lines. WT, wild type.

(C) and (D) AGPase large subunit 1 expression in fumarase (C) and MDH (D) lines.

(E) and (F) AGPase large subunit 2 expression in fumarase (E) and MDH (F) lines.

The values represent the means \pm SE of six individual plants. An asterisk indicates values determined by *t* test to be significantly different from the wild-type control ($P < 0.05$). Analyses were determined in different ripening stages. B-3, breaker 3 d postanthesis (DPA); B-1, breaker -1 DPA; B, breaker; B+3, breaker +3 DPA; B+1, breaker + 1 DPA. Individual lines are identified in the key on the graphs.

Ripening-Related Changes in the Transformants

Given the changes in pigment contents among the transgenics, which might indicate an alteration in the rate of ripening, we measured the expression levels of several known ripening-related genes by qRT-PCR. These included genes encoding proteins involved in cell wall modification and disassembly, including polygalacturonase, two expansins, and a xyloglucan endotransglucosylase/hydrolase, as well as the key starch biosynthetic enzyme AGPase and the core enzymes of ethylene synthesis, 1-aminocyclopropane-1-carboxylate oxidase (ACC oxidase) and aminocyclopropane-1-carboxylate synthase (ACC synthase; see Supplemental Figure 6 online). Most of the genes showed similar qualitative patterns of transcript accumulation,

and while some quantitative differences were apparent, they were within the range of typical intercultivar variation that we have previously observed (data not shown). Importantly, the expression of the cell wall-related genes was not dramatically repressed, as is the case for ripening-impaired mutants, such as *rin* and *nor*, where expression is generally undetectable (Maclachlan and Brady, 1994; Rose et al., 1997, 2003; Brummell and Harpster, 2001; Eriksson et al., 2004). Furthermore, the transgenics did not consistently show opposite patterns in the expression of any of these genes or those involved in starch or ethylene biosynthesis.

To complement this expression analysis, we investigated cell wall properties of the wild-type and transgenic fruit, specifically by evaluating sugar composition and pectin polymer size in

Table 5. Redistribution of Radiolabel after Incubation in [U¹⁴C]Glucose and Absolute Fluxes in Pericarp Discs of the Mitochondrial Fumarase and MDH Lines Isolated from Green Fruits Harvested 35 DAF

Parameter	Wild Type	F4	F6	M14	M21
	Bq g ⁻¹ FW				
Uptake	1595.7 ± 90.1	1078.7 ± 164.4	1566 ± 115.7	1322.3 ± 43.4	1515.7 ± 34.7
Metabolized	1411.2 ± 80.2	979.5 ± 149.3	1458.8 ± 103	1143.2 ± 41.5	1325.6 ± 25.1
Label incorporated in:	Bq g ⁻¹ FW				
Suc	1205.3 ± 71.7	715 ± 97.3	1047.2 ± 13.9	987.5 ± 67.2	1192.2 ± 42
Organic acids	23.12 ± 1.53	19.97 ± 3.53	19.13 ± 3.29	19.57 ± 0.66	23.58 ± 2.33
Amino acids	22.12 ± 1.3	19.29 ± 3.39	27.78 ± 8.72	23.02 ± 1.67	22.96 ± 2.4
Starch	20.27 ± 3.02	21.28 ± 3.64	28.15 ± 4.61	20.69 ± 1.32	20.11 ± 0.99
Protein	0.3 ± 0.14	0.31 ± 0.03	0.23 ± 0.09	0.67 ± 0.55	0.21 ± 0.1
Cell wall	12.86 ± 1.11	13.58 ± 2.13	17.85 ± 2.03	12.39 ± 0.48	14.7 ± 1.17
Phosphates esters	18.37 ± 1.15	19.62 ± 1.01	15.09 ± 2.47	14.24 ± 0.77	17.85 ± 2.37
	Bq nmol ⁻¹				
Specific activity of hexose phosphates	0.18 ± 0.02	0.26 ± 0.01	0.24 ± 0	0.21 ± 0.04	0.23 ± 0.03
Metabolic fluxes	nmol Hexose Equivalents g ⁻¹ FW				
Suc synthesis	9643.6 ± 961.74	5653.5 ± 962.5	6621.3 ± 287.6	8076.8 ± 1908.7	7826.3 ± 983.7
Starch synthesis	158.79 ± 10.32	185.96 ± 6.62	215.18 ± 14.79	125.28 ± 4.27	135.09 ± 12.3
Cell wall synthesis	102.37 ± 10.13	84.2 ± 12.38	132.74 ± 1.7	100.09 ± 16.56	103.47 ± 10.33
Protein synthesis	2.19 ± 0.9	2.02 ± 0.17	1.93 ± 0.21	5.89 ± 2.13	1.44 ± 0.46
Glycolytic	1710 ± 352.3	822.1 ± 3.4	1390.8 ± 43.4	1065.1 ± 9.9	856.7 ± 153.2
Ratios					
Starch/Suc	0.019 ± 0	0.039 ± 0.01	0.037 ± 0	0.014 ± 0	0.016 ± 0
Starch/Glycolysis	0.101 ± 0.02	0.211 ± 0.01	0.154 ± 0.01	0.118 ± 0	0.165 ± 0.02

Absolute rates of flux were calculated from the label incorporation data using the specific activity of the hexose-P pool to account for isotopic dilution factors. Values are presented as mean ± SE of determinations on three individual plants per line. Boldface type indicates values that were determined by the *t* test to be significantly different (*P* < 0.05) from the wild type. FW, fresh weight.

isolated cell walls. We performed these analyses for two reasons. First, in a previous study, we documented that inhibition of the TCA cycle resulted in a restriction of cell wall biosynthesis (Araújo et al., 2008); second, the decreased levels of minor sugars in green fruits of the transgenics described here may have been indicative of changes in cell wall composition. Cell wall monosaccharide analysis of wild-type fruit and pooled material from all three lines of MDH or fumarase plants revealed that this was essentially unaltered (see Supplemental Figure 7 online). Moreover, evaluation of pectin polymer size revealed no differences between the wild-type and transgenic lines (data not shown).

When taken together, these analyses indicate little difference in ripening-related processes per se or cell wall properties between the lines.

Postharvest Characteristics of the Transgenic Lines

Having established that the transformants exhibited an altered chemical composition, but no major difference in ripening-related cell wall characteristics, we also examined two aspects fruit physiology that are typical of overripening and that have great commercial importance: postharvest desiccation and susceptibility to microbial infection. Transpirational water loss from transgenic and wild-type fruit was assessed by measuring weight reduction over a 20-d period in fruits removed from the vine at the red ripe stage (Figure 5). Fruit from the MDH lines lost more water and showed clear signs of desiccation more rapidly than those of the wild type (Figure 5A), while in contrast, the

fumarase lines lost water more slowly (Figure 5B). These differences and consequent fruit shriveling are shown in the representative photos of wild-type and MDH lines taken 15 d after detachment of the fruit from the vine (Figure 5C) and of wild-type and fumarase lines taken 22 d after detachment (Figure 5D).

During storage and overripening, it was observed that fruit of the MDH-deficient genotypes were more susceptible to infection by opportunistic fungal pathogens than those of the wild type, while fruit of fumarase-deficient genotypes were less susceptible (a representative photograph is given in Supplemental Figure 8 online). Given this, we also assessed the resistance of the transgenic fruits to fungal infection in a more controlled environment by ectopically applying spores of the fungus *Botrytis cinerea* to the surface of red-ripe fruit of the wild-type and transgenic lines. To afford a large sample size, fruit were pooled from different plants within the transgenic line. While the transgenic fumarase, line F6, and wild-type fruit displayed similar levels of infection (that of F4 was significantly lower than the wild type), those from the MDH lines exhibited almost double the extent of infection (Figure 6).

DISCUSSION

Effect of Altered Mitochondrial Malate Metabolism on Fruit Respiration

Malate has long been implicated in the physiology of fruit ripening (Lance et al., 1967; Jeffery et al., 1984; Goodenough

Table 6. Metabolic Fluxes after Incubation in Malate

Parameter	Malate Concentration (mM)				
	0	10	30	50	70
	Bq g ⁻¹ FW				
Uptake	542.89 ± 36.95	479.05 ± 33.00	434.58 ± 25.62	442.93 ± 28.59	407.17 ± 30.49
Metabolized	435.30 ± 20.44	408.05 ± 23.19	371.99 ± 18.88	368.43 ± 27.82	342.79 ± 30.28
Redistribution of radiolabel	% of That Assimilated				
CO ₂	1.19 ± 0.48	1.16 ± 0.50	1.28 ± 0.74	1.06 ± 0.59	1.08 ± 0.56
Organic acids	15.27 ± 2.33	14.84 ± 1.32	16.27 ± 2.16	14.63 ± 1.22	15.28 ± 1.72
Amino acids	7.56 ± 1.38	7.32 ± 1.60	7.10 ± 1.49	7.35 ± 0.72	7.91 ± 0.74
Suc	11.92 ± 0.97	11.66 ± 0.37	11.67 ± 0.59	11.32 ± 0.39	11.24 ± 0.63
Starch	21.39 ± 0.81	19.42 ± 0.91	17.59 ± 1.27	17.05 ± 2.26	15.93 ± 2.11
Protein	4.20 ± 0.15	4.61 ± 0.26	4.38 ± 0.37	4.26 ± 0.12	4.46 ± 0.13
Cell wall	24.05 ± 1.67	24.21 ± 1.09	23.64 ± 1.38	25.83 ± 1.98	25.19 ± 2.09
Fru	6.27 ± 1.24	6.58 ± 1.02	6.73 ± 1.27	6.17 ± 1.17	6.14 ± 1.14
Phosphates esters	10.86 ± 1.36	12.60 ± 1.49	13.42 ± 1.12	14.03 ± 0.87	15.34 ± 2.33
Specific activity of	Bq nmol ⁻¹				
hexose phosphates	0.65 ± 0.05	0.63 ± 0.04	0.57 ± 0.03	0.65 ± 0.06	0.59 ± 0.05
Metabolic fluxes	nmol Hexose Equivalents g ⁻¹ FW h ⁻¹				
Starch synthesis	73.74 ± 8.07	63.72 ± 7.13	57.53 ± 6.18	51.79 ± 8.27	46.94 ± 5.27
Suc synthesis	105.31 ± 7.31	68.45 ± 7.91	65.81 ± 4.19	61.12 ± 4.42	70.66 ± 6.47
Glycolytic	99.52 ± 24.84	85.84 ± 10.42	86.27 ± 9.17	68.93 ± 3.05	97.25 ± 4.75
Amino acids synthesis	25.76 ± 6.60	18.12 ± 2.74	20.17 ± 3.65	19.17 ± 1.41	26.33 ± 3.04
Cell wall synthesis	84.48 ± 3.34	78.93 ± 6.06	87.63 ± 6.42	67.19 ± 8.02	77.33 ± 5.08
Organic acids synthesis	54.14 ± 6.26	49.06 ± 7.75	48.38 ± 6.67	35.60 ± 2.89	50.96 ± 6.71
Protein synthesis	30.13 ± 2.97	29.82 ± 1.56	26.73 ± 2.70	22.79 ± 0.86	28.98 ± 1.72

Redistribution of radiolabel following incubation in [¹⁴C] glucose and absolute fluxes in pericarp discs of the wild type isolated from green fruits harvested 35 DAF. Values are presented as mean ± SE of determinations on three replicates per concentration. Boldface type indicates values that were determined by the *t* test to be significantly different (*P* < 0.05) from the control. FW, fresh weight.

et al., 1985; Carrari et al., 2006); however, this is based primarily on indirect, correlative evidence, and the exact nature of its role in these organs has been somewhat unclear. To directly address the importance of this metabolite, we comprehensively characterized two sets of transgenic tomato lines in which the fruit malate content was reciprocally altered. These studies provided evidence for the importance of fruit mitochondrial metabolism in mediating redox regulation of plastidial starch and pigment metabolism, as well as alterations in total soluble solid content in red-ripe fruits and aspects of postharvest physiology.

As would be anticipated from constitutive alteration of fumarate and MDH (Nunes-Nesi et al., 2005, 2007), fruit-specific antisense of these enzymes resulted in reciprocal effects on malate content, with the fumarase lines displaying a mild decrease and the MDH lines an increase. Feeding experiments, involving incubation in positionally labeled glucoses, suggested that respiration was slightly differentially affected in the transgenics, with the fumarase lines displaying little alteration in the relative rates of the various routes of carbohydrate oxidation, whereas the MDH lines displayed higher flux through the reactions catalyzed by either pyruvate dehydrogenase, malic enzyme, or both. This can be surmised from the decreased C1/C3,4 ratios displayed by these lines since carbon release from the C3,4 position occurs via decarboxylation catalyzed by these enzymes.

That said, a more complete evaluation of the respiratory flux suggested that this was mildly reduced in both transgenic sets, although only significantly so in line F4. Further information

concerning respiratory metabolism can be inferred from the metabolite profiles; however, it is important to note that the mitochondrial pools of the organic acids only account for a small proportion of the total cellular pools (Stitt et al., 1989; ap Rees and Hill, 1994). It is notable that in addition to the clearly opposite trends in the levels of malate and fumarate, the green fruits of both transformants displayed lower levels of succinate, while the levels of citrate and isocitrate were also depressed in the fumarase lines. Despite these changes, the levels of ATP and ADP generally remained constant in red and green fruit of the fumarase lines; conversely, the green fruit of the MDH lines were characterized by decreased levels of ATP and a reduced ATP:ADP ratio.

However, it is important to note that similar changes were not apparent in the red fruit of this genotype. Since the rate of respiration increases during fruit ripening (Chalmers and Rowan, 1971; Woodrow and Rowan, 1979; Flores et al., 2006), the altered levels of adenylates in green fruit are more likely to be due to increased biosynthetic activities at this stage, rather than a decrease in ATP production per se, which would likely be more evident in the red fruit. In evaluation of the other major products of the TCA cycle, the reducing equivalents displayed similar patterns of change in both transgenic sets. Furthermore, several of the TCA cycle-derived amino acids were reduced in the red fruit of both sets of transgenics, suggesting a reduction in the anapleurotic capacity of the cycle (Sweetman et al., 2009). When taken together, these results suggest that, similar to the situation observed in tomato leaves, deficiency in the activities of MDH

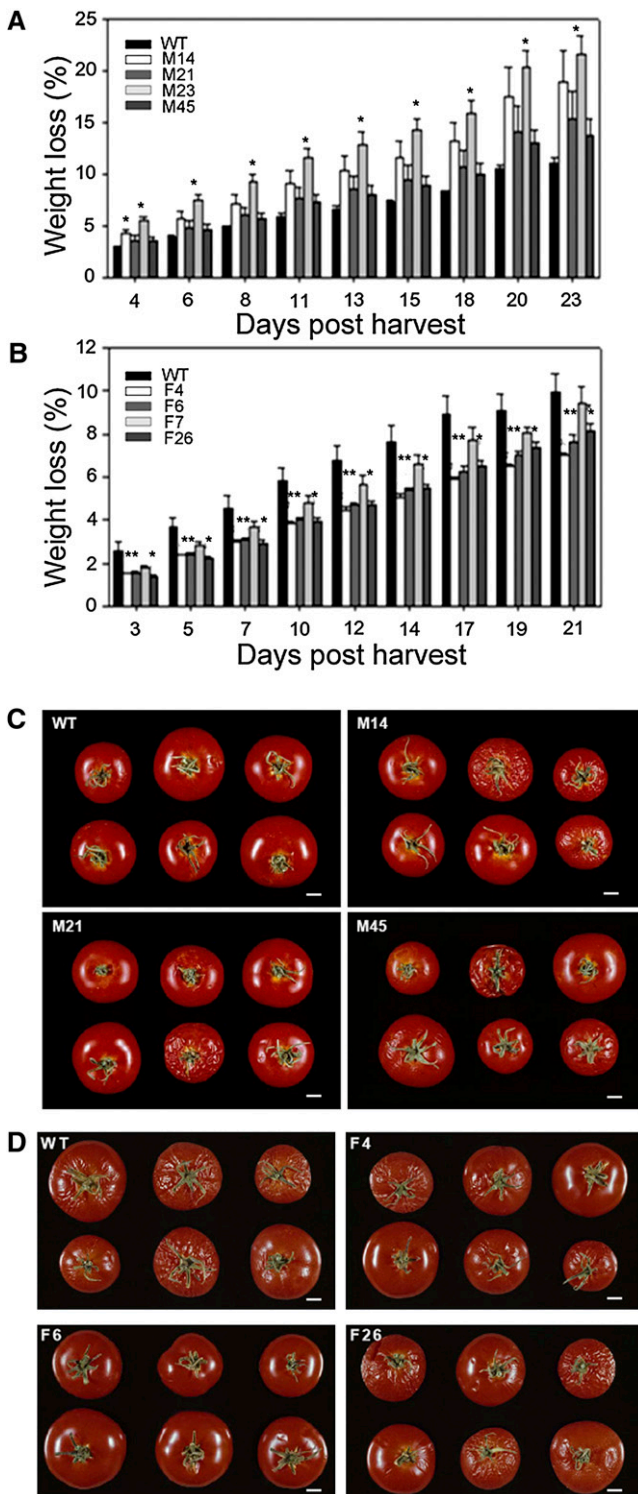


Figure 5. Postharvest Transpirational Water Loss of Fruits in the Anti-sense Fumarase and MDH Lines.

(A) and (B) Percentage of weight loss from detached fruits of MDH (A) and fumarase (B) lines over a 20-d period after reaching the red-ripe stage. WT, wild type.

(C) and (D) Representative photos of MDH (C) and fumarase (D) fruits 15

and fumarase do not dramatically effect respiration and hint that compensatory mechanisms are induced that ameliorate the situation, such as the increased activity of the malic enzyme (Drincovich et al., 2001; Fernie et al., 2004a).

Effect of Altered Mitochondrial Malate Metabolism on Starch Biosynthesis and Total Soluble Solids Content

Detailed analysis of the flux experiments revealed that while changes in respiratory metabolism were relatively minor, changes in the rate of starch biosynthesis were considerable. Furthermore, given the transitory nature of starch accumulation in tomato fruit (Robinson et al., 1988; Wang et al., 1993; Beckles et al., 2001), there were consequently large differences in the levels of soluble sugars at the red ripe stage. These data thus support the contention that active starch accumulation is an important contributory factor in determining the soluble solids content of mature fruit (Dinar and Stevens, 1981; Schaffer and Petreikov, 1997; Baxter et al., 2005).

Studies over the last 20 years concerning starch metabolism in potato cumulatively provided a deep understanding of the regulation and control of this pathway (Geigenberger et al., 2004; Smith, 2008). They suggest that the import and metabolism of adenylates (Tjaden et al., 1998; Regierer et al., 2002) as well as the reaction catalyzed by AGPase (Müller-Röber et al., 1992; Stark et al., 1992; Geigenberger et al., 1999; Sweetlove et al., 1999) are critical control points of the pathway. Regulation of the AGPase reaction has been very well characterized for several years. The enzyme is subject to transcriptional regulation, with expression being increased by sugars (Müller-Röber et al., 1990) and decreased by nitrate and phosphate (Nielsen et al., 1998). In addition, AGPase is exquisitely sensitive to allosteric regulation, being activated by 3PGA and inhibited by inorganic phosphate (Sowokinos, 1981; Sowokinos and Preiss, 1982). More recently, both in vitro and in vivo studies have demonstrated that AGPase is also redox regulated, being more active in the monomeric state (Fu et al., 1998; Tiessen et al., 2002), and other evidence suggests a role for trehalose-6-phosphate in determining the in vivo activation state (Kolbe et al., 2005; Lunn et al., 2006; Michalska et al., 2009).

In this study, a strong correlation was observed between the cellular malate and starch concentrations, and it was demonstrated that this was mechanistically linked to an altered redox status of the AGPase reaction. We could rule out major additional regulation at the transcriptional and allosteric levels; however, the maximal catalytic activity was enhanced, suggesting the operation of another mechanism that affects the AGPase protein levels. Intriguingly, the data presented here are analogous to those previously described for transgenic potato lines deficient in the expression of NAD-malic enzyme (Jenner et al., 2001), with

and 22 d after detaching from the vine.

Values are presented as mean \pm SE of determinations on six to nine fruits per line. Asterisks indicate values that were determined by the *t* test to be significantly different ($P < 0.05$) from the wild type. Individual lines are identified in the key on the graphs. Bar = 1 cm.

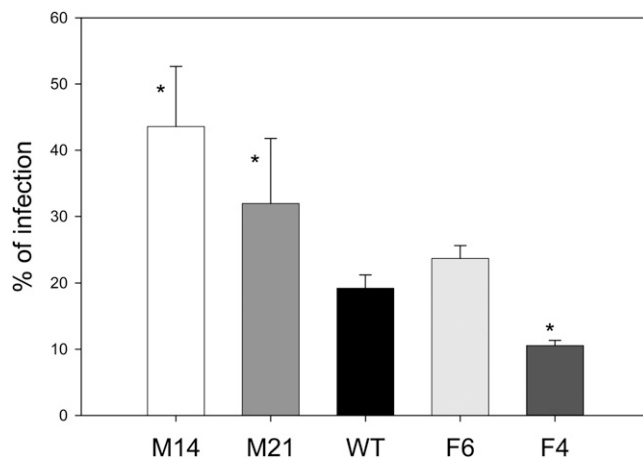


Figure 6. Microbial Infection of Wild-Type and Transgenic Fruits.

Percentage of fruits infected by *B. cinerea* in the antisense mitochondrial fumarase (Fum) and MDH lines after harvest and storage at 100% humidity at room temperature, 3 d after inoculation. Values are presented as mean \pm SE of determinations on 60 individual fruits per line. Asterisks indicate values that were determined by the *t* test to be significantly different ($P < 0.05$) from the wild type.

the exception that modification of starch content in tomato is clearly transient. Here, we demonstrated that alterations in mitochondrial malate metabolism have strong effects on starch biosynthesis in the amyloplast and, hence, influence agronomic yield. The observations described here have led us to propose a model in which starch metabolism influences fruit soluble sugar content, ripening, and postharvest physiology (Figure 7). This model synthesizes all of the phenotypes described in our study. It is evident that the genotypes studied here do not display dramatically elevated expression of the AGPase transcripts, but rather show altered overall activity and redox-dependent phenotypes. It thus seems likely that alterations in starch biosynthesis, within the genotypes, are set in part by alterations in posttranscriptional regulation of the reaction catalyzed by AGPase. The link between malate and redox regulation is by no means unprecedented, given that many studies have demonstrate the importance of malate in coordinating organellar metabolism (Scheibe, 1991, 2004). The discovery that altering mitochondrial malate metabolism influences the plastidial redox status was further confirmed by the observed alteration in the activation state of the plastidial MDH.

Effect of Altered Mitochondrial Malate Metabolism on Plastidial Pigment Biosynthesis and Ripening Behavior

Starch biosynthesis is not the only plastidial pathway modulated by redox status, and there is considerable evidence for its role in the regulation of tomato fruit pigment biosynthesis. Several of the biosynthetic enzymes, such as carotene *cis*-transisomerase, β -carotene hydroxylase, and zeaxanthin epoxidase, are redox regulated either at the transcriptional or allosteric levels (Woitsch and Römer, 2003; Isaacson et al., 2004). Furthermore, the recent

finding that a mutation of the subunit M of the tomato plastidial NADH dehydrogenase complex of tomato results in altered carotenoid biosynthesis (Nashilevitz et al., 2010) is in keeping with this finding. Here, we found minor yet opposing changes in the levels of several of the pigments, including chlorophyll *a* and *b*, lycopene, β -carotene, neoxanthin, and violaxanthin (see Supplemental Tables 14 and 15 online), in the absence of major changes in genes associated with the ripening process per se.

Impact of Altered Mitochondrial Malate Metabolism on Postharvest Physiology and Pathogen Resistance

In addition to altered cellular metabolism and the other ripening-related changes described above, we observed that the transgenic fruits showed differences in postharvest transpirational water loss and susceptibility to microbial infection. To summarize, the rates of water loss, consequent wrinkling, and susceptibility to fungal infection were greater in the MDH lines compared with wild-type fruits, while the converse was seen in the fumarate lines. Interestingly, as with the recently described *delayed fruit deterioration* mutant (Saladié et al., 2007), these differences showed no apparent association with typical ripening-related cell wall disassembly, which was indistinguishable between transgenic and wild-type fruits. Thus, while recent studies have indicated a strong link between cell wall degradation and susceptibility to *B. cinerea* (Cantu et al., 2008, 2009), our results suggest that the susceptibility of the MDH line is mediated via a different mechanism. Intriguingly, malate is one of the tricarboxylic acids found in the apoplast following elicitation of the pathogen response in both French bean (*Phaseolus vulgaris*) and *Arabidopsis thaliana* (Bolwell et al., 2002; Bolwell and Daudi, 2009), suggesting a potential role for the metabolite in this process. However, the fact that the MDH lines are likely to display elevated levels of malate suggests that this increase is most likely merely a consequence of increased TCA cycle activity under such conditions. A recent study suggested that cutin, the predominant polymer of the fruit cuticle, is highly important in offering microbial resistance but is not universally linked to transpirational water loss (Isaacson et al., 2009). Moreover, biomechanical analysis of cuticles from the fumarase and MDH lines showed no difference compared with those from wild-type fruit (data not shown). We therefore suggest that the altered postharvest traits were not likely a consequence of substantially altered cuticle structure. We cannot, as yet, explain the mechanism underlying the observed changes in either feature of the transgenic lines. However, the fact that the red-ripe fruit contain contrasting levels of soluble sugars suggests that osmotic potential may be a contributing factor that links the altered mitochondrial function to the water loss phenotype and consequent differences in pathogen susceptibility that were observed postharvest. A more detailed analysis of postharvest physiology of this material will likely allow us to delimit the underlying mechanisms of these changes in the near future.

Conclusion

Following an extensive, descriptive metabolic study of tomato fruit development (Carrari et al., 2006), we identified malate as a

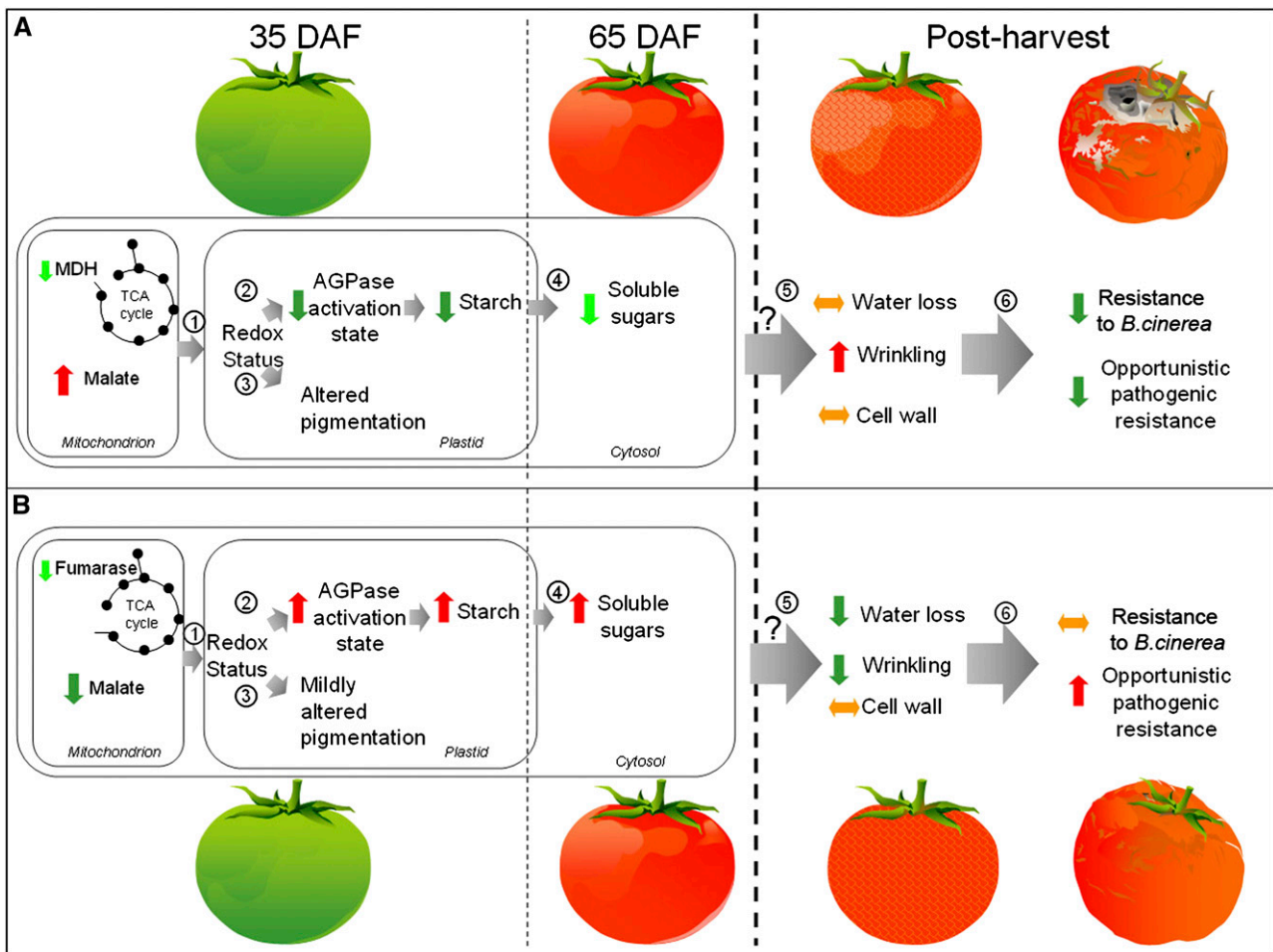


Figure 7. Model of the Influence of Mitochondrially Derived Malate on Tomato Fruit Starch, Soluble Sugar Content, Postharvest Shelf Life, and Bacterial Infection.

Data presented from analyses of the transgenic lines characterized in this article are schematically summarized in relation to the wild type (WT). Mitochondrial MDH lines (**[A]**; increased malate); fumarase lines (**[B]**; decreased malate). The same ripening and postharvest sequence is presented for both transgenic sets. (1) Alterations in mitochondrial redox status are transmitted, either within the same cell type or from adjacent tissues, to the plastid via the malate valve as described by Scheibe (2004). (2) Altered plastidial redox status results in a reduced (MDH) or enhanced (fumarase) activation state of the reaction catalyzed by AGPase (as well as similar changes in the activation state of the plastidial MDH); whether this is mediated by the thioredoxin or the NTR-C pathway is currently unknown. (3) This leads to redox-mediated alterations in pigment biosynthesis during ripening. (4) Starch is rapidly broken down, leading to a reduced soluble solid content in red-ripe fruit in the MDH lines and an increased soluble solid content in the fumarase lines. (5) Potentially as a result of differences in cellular osmolarity, the transgenic sets oppositely display an increased water loss and wrinkling (MDH) or a decreased water loss and wrinkling (fumarase) that appears to be cell wall independent. (6) These changes in water loss and wrinkling correlate positively to the rate of opportunistic pathogen infection in the transgenic sets, while the MDH lines are increasingly susceptible to *B. cinerea* infection.

potentially important regulatory metabolite. Here, we demonstrated that alterations in the level of malate resulted in dramatic effects on transitory starch metabolism: lines displaying low malate content showed an increased flux to, and accumulation of, starch, whereas those displaying high levels of malate showed the opposite effect. Detailed analysis of this phenomena revealed that it was due to alterations in the activation state of AGPase, caused by alterations in the redox status of the plastid. Nevertheless, it would appear that mitochondrial metabolism is able to dramatically influence plastidial metabolism in the devel-

oping fruit. Further support for the role of malate in this process was provided by the ability to phenocopy the MDH lines using experiments in which the metabolic fate of radiolabel was determined following incubation of green pericarp discs in [^{14}C] glucose in the presence or absence of varying concentrations of malate. On progression through ripening, the (lack of) accumulation of transitory starch was reflected by a decrease of soluble sugars in the MDH lines and an increase in the fumarase lines. At the postharvest stage, the transgenic sets continue to exhibit opposing phenotypes, with the MDH lines being characterized

by elevated water loss and wrinkling, while fumarase lines showed the opposite behavior with respect to the wild type. Wholly consistent with these changes were the observed differences in opportunistic infection and the increased susceptibility of the MDH lines to *B. cinerea*. In summary, the data presented here confirmed our hypothesis that altering mitochondrial malate metabolism would have far-reaching metabolic and developmental consequences on tomato fruit ripening.

METHODS

Materials

Tomato (*Solanum lycopersicum*) cv Moneymaker seeds were obtained from Meyer Beck. The seeds were germinated on Murashige and Skoog media (Murashige and Skoog, 1962) containing 2% (w/v) Suc and were grown in a growth chamber (250 $\mu\text{mol photons m}^{-2} \text{s}^{-1}$, 22°C) under a 16-h-light/8-h-dark regime before transfer into the greenhouse, where they were grown in parallel with a minimum of 250 $\mu\text{mol photons m}^{-2} \text{s}^{-1}$, 22°C, under a 16-h/8-h daylight period. The stage of fruit development was followed by tagging the truss upon appearance of the flower. Unless otherwise stated, samples were only harvested at two time points, 35 and 65 DAF; however, a range of other samples were taken at a number of time points around the breaker stage. Unless stated otherwise, all chemicals, cofactors, or enzymes were purchased either from Sigma-Aldrich Chemical Company or from Merck KGaG.

Generation of Transgenic Plants

Plants expressing mitochondrial MDH or fumarase in a fruit-specific manner in the antisense orientation were generated by cloning a 1860-bp fragment of the tomato fumarase gene or a 996-bp fragment of tomato mMDH into the vector pBINAR (Liu et al., 1990) between the B33 patatin promoter and the *ocs* terminator. These constructs were independently introduced into plants by an *Agrobacterium tumefaciens*-mediated transformation protocol, and plants were selected and maintained as described in the literature (Taubberger et al., 2000). Initial screening of 16 lines, for plants containing the tomato fumarase antisense construct and 40 lines, for plants containing tomato mMDH, was performed at the level of the respective enzyme activities. These screens allowed the selection of six lines per construct, which were taken to the next generation. Total activities were confirmed for the second harvest of these lines, after which four lines per construct were chosen for detailed physiological and biochemical analyses.

Enzyme Analyses

Enzymes were extracted from pericarp tissue as described previously (Taubberger et al., 2000; Steinhauser et al., 2010) and assayed as described (Gibon et al., 2004; Nunes-Nesi et al., 2005), with the exception that they were optimized for tomato fruit.

Immunodetection of AGPase Protein

Frozen plant material was extracted directly with 1 \times sample buffer (62.5 mM Tris-Cl, pH 6.9, 2% SDS, 10% glycerol, and 0.02% bromophenol blue, supplemented with 1 mM benzimidazole, 1 mM ϵ -amino caproic acid, 1 mM EDTA, and 1 mM EGTA) that had been degassed either by boiling the buffer or using an argon line. For every milligram of plant material, 5 μL of buffer was added. After centrifugation of the sample for 30 s at 10,000g, the supernatant was boiled immediately for 5 to 10 min. To a part of the sample, 4 mM DTT was added (+DTT), and the rest was used as prepared

(DTT). Equal amounts of both samples were loaded onto a 10% acrylamide gel containing SDS (Laemmli, 1970) and separated. After transfer of the proteins to polyvinylidene difluoride, the membrane was incubated with a rabbit antibody raised against the brittle-2 protein (AGPB) from maize (*Zea mays*; Giroux and Hannah, 1994) followed by a peroxidase-conjugated anti-rabbit secondary antibody (Bio-Rad). Peroxidase activity was detected on x-ray film by enhanced chemiluminescence exactly as described by Tiessen et al. (2002).

Metabolite Profiling

Cellular metabolites levels were analyzed exactly as outlined by Roessner et al. (2001), with the exceptions that initial parameters taken were optimized for tomato following the method of Roessner-Tunali et al. (2003) and that additional compounds were detected by application of the mass spectral library approach described by Schauer et al. (2005). The levels of starch, Suc, Fru, and Glc in the fruit tissue were determined exactly as described previously (Fernie et al., 2001). Pigments were measured as described by Carrari et al. (2006). Malate and fumarate were measured as detailed by Nunes-Nesi et al. (2007). NAD, NADP, NADH, and NADPH were determined as previously described (Gibon and Larher, 1997; Schippers et al., 2008). Adenylates were measured by HPLC as detailed by Fernie et al. (2001). Unless described otherwise, all measurements were performed on pericarp tissue. However, we also profiled columnella, medula, and locular tissues.

RNA Extraction and Quantification for qRT-PCR Analysis

The RNA and qRT-PCR were determined as described by Zanol et al. (2009). Expression of expansin 1 (*Le EXP1*), expansin precursor (*EXPA3*), 1-aminocyclopropane-1-carboxylate oxidase (*SI ACO1*), ethylene-forming enzyme (*SI ACO3*), ACC synthase 2 (*Le ACS2*), 1-aminocyclopropane-1-carboxylate synthase (*SI ACS4*), ADP-glucose pyrophosphorylase small subunit (*AGPase*), xyloglucan endotransglucosylase/hydrolase (*SI XTH5*), polygalacturonase (*Le PG1*), AGPase large subunit 1 (*AGPaseL1*), and AGPase large subunit 2 (*AGPaseL2*) was analyzed by real-time qRT-PCR using the fluorescent intercalating dye SYBR Green in an iCycler detection system (Bio-Rad) as described by Schaarschmidt et al. (2006). Relative quantification of the target expression level was performed using the comparative Ct method. The following primers were used: for analysis of *Le EXP1*, transcript levels forward 5'-TACCAATTTCTGCCACCAAT-3' and reverse 5'-GGTTACACCAGCCACCATTTG-3'; for *SI ACO1*, forward 5'-AAATCATGAAGGAGTTTGTGATAAA-3' and reverse, 5'-TTTTCACACAGCAAATCCAACAG-3'; for *SI ACO3*, forward 5'-ACGGGAAGTACAA-GAGCGTGAT-3' and reverse 5'-CTAGTGACATCCGAGTCCCATCT-3'; for *Le ACS2*, forward 5'-TGGAGAAAACAAGAGGAGGAAGA-3' and reverse 5'-GGCACCACCAGCCATAACA-3'; for *SI ACS4*, forward 5'-CCATCTTGTGGCGACGAAATA-3' and reverse 5'-CGATGCTAACGAA-TTTTGGAGAA-3'; for *AGPase*, forward 5'-TAAATCGCCACCTTTCACGG-3' and reverse 5'-CGGACTTTGTGAGCAGCAAG-3'; for *SIXTH5*, forward 5'-GGATTCAGCCATCTCTTTGGTG-3' and reverse 5'-GAACCTGAACCTGTGTTTTGG-3'; for *EXPA3*, forward 5'-TTTGCGGAGCTTGCTTTGAA-3' and reverse 5'-GGAGCACAAAAATTCGTTGAG-3'; for *Le PG1*, forward 5'-GGCAATGGACAAGTATGGTGG-3' and reverse 5'-CAGAAGGT-TAAGGCCGTTGGT-3'; for *AGPase L1*, forward 5'-GATTATATGGAGT-TGGTGCAGAACC-3' and reverse 5'-ACCAGCCCAAATCTGATGCT-3'; and for *AGPase L2*, forward 5'-GTCGGGCCAAACACTAAGATACA-3' and reverse 5'-TCAGCTTCTTCAACACCTTGCTT-3'. To normalize genes, expression was used the constitutively expressed elongation factor 1- α (GenBank accession number X14449) and ubiquitin3 (GenBank accession number X58253) using the following primers: forward, 5'-ACCACGAAGCTCTCCAGGAG-3', and reverse, 5'-CATTGAACCCAAACATTGTC-ACC-3', Schaarschmidt et al. (2006) for elongation factor 1- α ; and forward,

5'-AGGTTGATGACACTGGAAGGTT-3', and reverse, 5'-ATCGCCTC-CAGCCTTGTGTA-3' for ubiquitin3 (Wang et al., 2008).

Measurement of Respiratory Parameters

Estimations of the TCA cycle flux on the basis of $^{14}\text{CO}_2$ evolution were performed following incubation of isolated pericarp discs in 10 mM MES-KOH, pH 6.5, containing 2.32 KBq mL^{-1} of $[1-^{14}\text{C}]$ -, $[3:4-^{14}\text{C}]$ -, or $[6-^{14}\text{C}]$ glucose following previously described protocols (ap Rees and Beevers, 1960; Nunes-Nesi et al., 2005). $^{14}\text{CO}_2$ evolved was trapped in KOH and quantified by liquid scintillation counting.

Incubation of Plant Material with $[\text{U}-^{14}\text{C}]$ Glucose

Developing fruits were removed at 35 DAF, and a 10-mm-diameter latitudinal core was taken. Both cuticular and locular tissues were removed, and the residual pericarp material was sliced into 2-mm slices and washed three times in fresh incubation medium (10 mM MES-KOH, pH 6.5) and then incubated (eight discs in 5 mL of incubation medium containing $[\text{U}-^{14}\text{C}]$ glucose [$1.4 \text{ MBq mmol}^{-1}$]) to a final concentration of 10 mM. Samples were then incubated for 2 h before washing again three times in unlabeled incubation medium and freezing in liquid N_2 until further analysis. All incubations were performed in a sealed 100-mL flask at 25°C and shaken at 150 rpm. The evolved $^{14}\text{CO}_2$ was collected in 0.5 mL of 10% (w/v) KOH.

Fractionation of ^{14}C -Labeled Material

Tissue was fractionated as described by Fernie et al. (2001), with the exception that hexoses were fractionated enzymatically rather than using thin-layer chromatography. Labeled Suc levels were determined after a 4-h incubation of 200 μL of total neutral fraction with 4 units/mL of hexokinase in 50 mM Tris-HCl, pH 8.0, containing 13.3 mM MgCl_2 and 3.0 mM ATP at 25°C . For labeled Glc and Fru levels, 200 μL of neutral fraction were incubated with 1 unit/mL of glucose oxidase and 32 units/mL of peroxidase in 0.1 M potassium phosphate buffer, pH 6, for a period of 6 h at 25°C . After the incubation time, all reactions were stopped by heating at 95°C for 5 min. The label was subsequently separated by ion-exchange chromatography as described by Fernie et al. (2001). The rationale of these experiments is that hexose sugars will be converted to their respective hexose phosphates via the action of hexokinase leaving Suc as the only major component of the neutral fractionation. Since glucose oxidase specifically oxidizes Glc, but not Fru, forming D-gluconolactone, the difference between nonenzymatically treated neutrals and those treated with either hexokinase or glucose oxidase can be used to directly determine labeling in Suc or Glc and indirectly determine that in Fru. The reliability of these fractionation techniques have been thoroughly documented previously (Fernie et al., 2001; Carrari et al., 2006).

Cell Wall Analysis

Cell walls were prepared from 50 g of diced outer pericarp of wild-type and transgenic fruit (mature-green and red-ripe stages) by boiling the pericarp pieces in 95% ethanol for 30 min to prevent autolytic activity, as described by Huysamer et al. (1997). Subsequent steps in preparing crude cell wall samples (alcohol-insoluble solids [AISs]) were also as described by Huysamer et al. (1997), ending with two washes of the cell wall pellets with acetone and a final drying in a vacuum oven. Starch was removed by incubating 200 mg of AIS with 40 units each of α -amylase (from porcine pancreas; Sigma-Aldrich) and pullulanase (from *Bacillus acidopullulyticus*; Novozymes Biologicals) in 20 mL of Tris-HCl, pH 7.0, and 0.1% NaN_3 for 24 h. Neutral sugar composition of the AIS was determined by gas-liquid chromatography as described by Campbell

et al. (1990). Duplicate 2- to 3-mg samples of AIS were hydrolyzed in trifluoroacetic acid (TFA), and the trifluoroacetic acid-soluble fraction was converted to alditol acetates and analyzed by gas-liquid chromatography (Rose et al., 1998).

For the size-exclusion chromatography analysis, the AIS was treated with water and 50 mM cyclohexane diamine tetraacetic acid (Rose et al., 1998). The water and cyclohexane diamine tetraacetic acid-soluble materials (3 to 4 mg) were dissolved in 50 mM ammonium formate, pH 5.0 (500 μL) and centrifuged to remove insoluble material, and the soluble material analyzed by size-exclusion chromatography using a Superose-12 HR10/30 column (GE Healthcare). The column was eluted at 0.6 mL min^{-1} with 50 mM ammonium formate, pH 5, using a Dionex BioLc (Dionex). The eluant was monitored with a Knauer differential refractometer.

Water Loss Measurements

Six fruits from the wild-type and transgenic lines were detached at the red-ripe stage and kept at room temperature for over a 20-d period. Water loss per unit fruit surface area was calculated after measuring the weight decrease over time and measuring fruit dimensions.

Microbial Inoculation and Infection

Fruits from wild-type and both transgenic lines were detached from the vine at the red-ripe stage and were stored at room temperature in a moist container to assess opportunistic microbial infection exactly as described by Saladié et al. (2007). Red-ripe fruits from wild-type, MDH, and fumarase lines were inoculated with three concentrations of *Botrytis cinerea* (strain Del 11) spores (10^3 , 10^6 , and 10^8) by ectopic application onto the fruit surface. Fruits were stored in moist sealed boxes at room temperature as described by Saladié et al. (2007).

Statistical Analyses

The Student's *t* test was performed using the algorithm embedded into Microsoft Excel 2003. The term "significant" is used in the text only when the change in question has been confirmed to be significant ($P < 0.005$).

Accession Numbers

Sequence data from this article can be found in the GenBank/EMBL database under the following accession numbers: expansin 1 (Le *EXP1*, U82123), expansin precursor (*EXPA3*, AF059487), 1-aminocyclopropane-1-carboxylate oxidase (SI *ACO1*, EF501822), ethylene-forming enzyme (SI *ACO3*, X58885), ACC synthase 2 (Le *ACS2*, AY326958), 1-aminocyclopropane-1-carboxylate synthase (SI *ACS4*, M63490), ADP-glucose pyrophosphorylase small subunit (*AGPasa*, L41126), xyloglucan endotransglucosylase/hydrolase (SI *XTH5*, AY497475), polygalacturonase (Le *PG1*, X14074), AGPase large subunit 1 (*AGPaseL1*, U81033), AGPase large subunit 2 (*AGPaseL2*, U81034), mitochondrial MDH (*mMDH*, AY725474), and fumarase (Fum, SGN-U570526).

Supplemental Data

The following materials are available in the online version of this article.

Supplemental Figure 1. Screening of Total Fumarase and MDH Activity in Primary Fumarase and Malate Dehydrogenase Transformants in Extract of Tissue Sampled from Green Fruits 35 DAF.

Supplemental Figure 2. Total Malate Dehydrogenase and Fumarase Activities Determined in Young and Old Leaves.

Supplemental Figure 3. Total Fumarase Activity in Fumarase Lines in Different Fruit Tissues.

Supplemental Figure 4. Total Malate Dehydrogenase Activity in Malate Dehydrogenase Lines in Different Fruit Tissues.

Supplemental Figure 5. Evaluation of the Dimerization of AGPase after Incubation of Wild-Type Pericarp Discs in 50 mM Mannitol.

Supplemental Figure 6. Expression of Ripening-Related Genes of Wild-Type, Fumarase, and Malate Dehydrogenase Transgenic Lines.

Supplemental Figure 7. Composition of Cell Wall Neutral Sugars of Fruits in the Antisense Fumarase and Malate Dehydrogenase Lines.

Supplemental Figure 8. Opportunistic Microbial Infection of Fruits in the Antisense Mitochondrial Fumarase and Malate Dehydrogenase Lines.

Supplemental Table 1. Malate and Fumarate Content in Different Tissues of Fruits with 35 DAF from Wild-Type and Fumarase Antisense Plants

Supplemental Table 2. Malate and Fumarate Content in Different Tissues of Fruits with 35 DAF from Wild-Type and Malate Dehydrogenase Antisense Plants.

Supplemental Table 3. Starch Content in Different Tissues of Fruits with 35 DAF from Wild-Type and Fumarase Antisense Plants.

Supplemental Table 4. Starch Content in Different Tissues of Fruits with 35 DAF from Wild-Type and Malate Dehydrogenase Antisense Plants.

Supplemental Table 5. Comparison of Metabolic Levels from Pericarp Tissue of Fruits with 35 DAF from Wild-Type, Fumarase, and Malate Dehydrogenase Antisense Plants.

Supplemental Table 6. Comparison of Metabolic Levels from Columnela Tissue of Fruits with 35 DAF from Wild-Type, Fumarase, and Malate Dehydrogenase Antisense Plants.

Supplemental Table 7. Comparison of Metabolic Levels from Medula Tissue of Fruits with 35 DAF from Wild-Type, Fumarase, and Malate Dehydrogenase Antisense Plants.

Supplemental Table 8. Comparison of Metabolic Levels from Locula Tissue of Fruits with 35 DAF from Wild-Type, Fumarase, and Malate Dehydrogenase Antisense Plants.

Supplemental Table 9. Comparison of Metabolic Levels from Pericarp Tissue of Fruits with 65 DAF from Wild-Type, Fumarase, and Malate Dehydrogenase Antisense Plants.

Supplemental Table 10. Comparison of Metabolic Levels from Columnela Tissue of Fruits with 65 DAF from Wild-Type, Fumarase, and Malate Dehydrogenase Antisense Plants.

Supplemental Table 11. Comparison of Metabolic Levels from Medula Tissue of Fruits with 65 DAF from Wild-Type, Fumarase, and Malate Dehydrogenase Antisense Plants.

Supplemental Table 12. Comparison of Metabolic Levels from Locula Tissue of Fruits with 65 DAF from Wild-Type, Fumarase, and Malate Dehydrogenase Antisense Plants.

Supplemental Table 13. Comparison of Metabolic Levels of Breaker-3 DAF Stage Fruits from Wild-Type, Fumarase, and Malate Dehydrogenase Antisense Plants.

Supplemental Table 14. Comparison of Metabolic Levels of Breaker-1 DAF Fruits from Wild-Type, Fumarase, and Malate Dehydrogenase Antisense Plants.

Supplemental Table 15. Comparison of Metabolic Levels of Breaker Stage Fruits from Wild-Type, Fumarase, and Malate Dehydrogenase Antisense Plants.

Supplemental Table 16. Comparison of Metabolic Levels of Breaker +1 DAF Fruits from Wild-Type, Fumarase, and Malate Dehydrogenase Antisense Plants.

Supplemental Table 17. Comparison of Metabolic Levels of Breaker +3 DAF Fruits from Wild-Type, Fumarase, and Malate Dehydrogenase Antisense Plants.

Supplemental Table 18. Pigment Content during Fruit Development in the Mitochondrial Fumarase Lines.

Supplemental Table 19. Pigment Content during Fruit Development in the Mitochondrial Malate Dehydrogenase Lines.

ACKNOWLEDGMENTS

We thank Takayuki Tohge (Max-Planck-Institut für Molekulare Pflanzenphysiologie) for the time expended preparing the tomato pictures. We also thank Antje Lohmann (Max-Planck-Institut für Molekulare Pflanzenphysiologie) for pigment measurements. In addition, we acknowledge the excellent care of the plants by Helga Kulka (Max-Planck-Institut für Molekulare Pflanzenphysiologie). This research was partially supported by the European Commission (EU-SOL Project PI 016214; A.R.F. and M.-C.S.) by the ERA-NET TRIPTOP project funded by Deutschen Forschungsgemeinschaft (A.N.-N., A.R.F.), partially by the ERA-NET-financed project TomQML (S.N.O. and A.R.F.), by Coordenação de Aperfeiçoamento de Pessoal de Nível Superior and the Deutscher Akademischer Austausch Dienst (D.C.C.), partially by the Deutschen Forschungsgemeinschaft Project GE 878/5-1, 8-1 (P.G.), by National Science Foundation Grant DBI-0606595, and by the USDA Cooperative State Research, Education, and Extension Service (Grant 2006-3530417323 to J.R.).

Received October 16, 2009; revised November 10, 2010; accepted December 19, 2010; published January 14, 2011.

REFERENCES

- Alba, R., et al.** (2004). ESTs, cDNA microarrays, and gene expression profiling: Tools for dissecting plant physiology and development. *Plant J.* **39**: 697–714.
- ap Rees, T., and Beevers, H.** (1960). Pentose-phosphate pathway as a major component of induced respiration of carrot and potato slices. *Plant Physiol.* **35**: 839–847.
- ap Rees, T., and Hill, S.A.** (1994). Metabolic control analysis of plant metabolism. *Plant Cell Environ.* **17**: 587–599.
- Araújo, W.L., Nunes-Nesi, A., Trenkamp, S., Bunik, V.I., and Fernie, A.R.** (2008). Inhibition of 2-oxoglutarate dehydrogenase in potato tuber suggests the enzyme is limiting for respiration and confirms its importance in nitrogen assimilation. *Plant Physiol.* **148**: 1782–1796.
- Ballicora, M.A., Laughlin, M.J., Fu, Y., Okita, T.W., Barry, G.F., and Preiss, J.** (1995). Adenosine 5'-diphosphate-glucose pyrophosphorylase from potato tuber. Significance of the N terminus of the small subunit for catalytic properties and heat stability. *Plant Physiol.* **109**: 245–251.
- Barry, C.S., and Giovannoni, J.J.** (2006). Ripening in the tomato Green-ripe mutant is inhibited by ectopic expression of a protein that disrupts ethylene signaling. *Proc. Natl. Acad. Sci. USA* **103**: 7923–7928.
- Baxter, C.J., Carrari, F., Bauke, A., Overy, S., Hill, S.A., Quick, P.W., Fernie, A.R., and Sweetlove, L.J.** (2005). Fruit carbohydrate metabolism in an introgression line of tomato with increased fruit soluble solids. *Plant Cell Physiol.* **46**: 425–437.

- Beckles, D.M., Craig, J., and Smith, A.M. (2001). ADP-glucose pyrophosphorylase is located in the plastid in developing tomato fruit. *Plant Physiol.* **126**: 261–266.
- Bolwell, G.P., Bindschedler, L.V., Blee, K.A., Butt, V.S., Davies, D.R., Gardner, S.L., Gerrish, C., and Minibayeva, F. (2002). The apoplastic oxidative burst in response to biotic stress in plants: A three-component system. *J. Exp. Bot.* **53**: 1367–1376.
- Bolwell, G.P., and Daudi, A. (2009). Reactive oxygen species in plant-pathogen interactions. In *Reactive Oxygen Species in Plant Signaling, Signaling and Communication in Plants*, L.A. del Rio and A. Puppo, eds (Berlin, Heidelberg, Germany: Springer-Verlag), pp. 113–134.
- Bramley, P.M. (2002). Regulation of carotenoid formation during tomato fruit ripening and development. *J. Exp. Bot.* **53**: 2107–2113.
- Brummell, D.A., and Harpster, M.H. (2001). Cell wall metabolism in fruit softening and quality and its manipulation in transgenic plants. *Plant Mol. Biol.* **47**: 311–340.
- Butelli, E., Titta, L., Giorgio, M., Mock, H.P., Matros, A., Peterek, S., Schijlen, E.G.W.M., Hall, R.D., Bovy, A.G., Luo, J., and Martin, C. (2008). Enrichment of tomato fruit with health-promoting anthocyanins by expression of select transcription factors. *Nat. Biotechnol.* **26**: 1301–1308.
- Campbell, A.D., Huysamer, M., Stotz, H.U., Greve, L.C., and Labavitch, J.M. (1990). Comparison of ripening processes in intact tomato fruit and excised pericarp discs. *Plant Physiol.* **94**: 1582–1589.
- Cantu, D., Blanco-Ulate, B., Yang, L., Labavitch, J.M., Bennett, A.B., and Powell, A.L. (2009). Ripening-regulated susceptibility of tomato fruit to *Botrytis cinerea* requires NOR but not RIN or ethylene. *Plant Physiol.* **150**: 1434–1449.
- Cantu, D., Vincente, A.R., Greve, L.C., Dewey, F.M., Bennett, A.B., Labavitch, J.M., and Powell, A.L. (2008). The intersection between cell wall disassembly, ripening, and fruit susceptibility to *Botrytis cinerea*. *Proc. Natl. Acad. Sci. USA* **105**: 859–864.
- Cara, B., and Giovannoni, J.J. (2008). Molecular biology of ethylene during tomato fruit development and maturation. *Plant Sci.* **175**: 106–113.
- Carrari, F., Baxter, C., Usadel, B., Urbanczyk-Wochniak, E., Zanor, M.I., Nunes-Nesi, A., Nikiforova, V., Centero, D., Ratzka, A., Pauly, M., Sweetlove, L.J., and Fernie, A.R. (2006). Integrated analysis of metabolite and transcript levels reveals the metabolic shifts that underlie tomato fruit development and highlight regulatory aspects of metabolic network behavior. *Plant Physiol.* **142**: 1380–1396.
- Carrari, F., and Fernie, A.R. (2006). Metabolic regulation underlying tomato fruit development. *J. Exp. Bot.* **57**: 1883–1897.
- Carrari, F., Nunes-Nesi, A., Gibon, Y., Lytovchenko, A., Loureiro, M.E., and Fernie, A.R. (2003). Reduced expression of aconitase results in an enhanced rate of photosynthesis and marked shifts in carbon partitioning in illuminated leaves of wild species tomato. *Plant Physiol.* **133**: 1322–1335.
- Chalmers, D.J., and Rowan, K.S. (1971). The climacteric in ripening tomato fruit. *Plant Physiol.* **48**: 235–240.
- Davuluri, G.R., et al. (2005). Fruit-specific RNAi-mediated suppression of DET1 enhances carotenoid and flavonoid content in tomatoes. *Nat. Biotechnol.* **23**: 890–895.
- Dharmapuri, S., Rosati, C., Pallara, P., Aquilani, R., Bouvier, F., Camara, B., and Giuliano, G. (2002). Metabolic engineering of xanthophyll content in tomato fruits. *FEBS Lett.* **519**: 30–34.
- Dinar, M., and Stevens, M.A. (1981). The relationship between starch accumulation and soluble solids content of tomato fruits. *J. Am. Soc. Hortic. Sci.* **106**: 415–418.
- Drincovich, M.F., Casati, P., and Andreo, C.S. (2001). NADP-malic enzyme from plants: A ubiquitous enzyme involved in different metabolic pathways. *FEBS Lett.* **490**: 1–6.
- Eriksson, E.M., Bovy, A., Manning, K., Harrison, L., Andrews, J., De Silva, J., Tucker, G.A., and Seymour, G.B. (2004). Effect of the *Colorless non-ripening* mutation on cell wall biochemistry and gene expression during tomato fruit development and ripening. *Plant Physiol.* **136**: 4184–4197.
- Faurobert, M., Mihr, C., Bertin, N., Pawlowski, T., Negroni, L., Sommerer, N., and Causse, M. (2007). Major proteome variations associated with cherry tomato pericarp development and ripening. *Plant Physiol.* **143**: 1327–1346.
- Fernie, A.R., Carrari, F., and Sweetlove, L.J. (2004a). Respiratory metabolism: Glycolysis, the TCA cycle and mitochondrial electron transport. *Curr. Opin. Plant Biol.* **7**: 254–261.
- Fernie, A.R., Roscher, A., Ratcliffe, R.G., and Kruger, N.J. (2001). Fructose 2,6-bisphosphate activates pyrophosphate: fructose-6-phosphate 1-phosphotransferase and increases triose phosphate to hexose phosphate cycling in heterotrophic cells. *Planta* **212**: 250–263.
- Fernie, A.R., Trethewey, R.N., Krotzky, A.J., and Willmitzer, L. (2004b). Metabolite profiling: From diagnostics to systems biology. *Nat. Rev. Mol. Cell Biol.* **5**: 763–769.
- Flores, F.B., Sanchez-Ballesta, M.T., Bouzayen, M., Latche, A., and Pech, J.C. (2006). Mechanisms of fruit ripening: Retrospect and prospects. *Acta Hort.* **712**: 317–324.
- Foyer, C.H., Lelandais, M., and Harbinson, J. (1992). Control of the quantum efficiencies of photosystem-I and photosystem-2, electron flow, and enzyme activation following dark-to-light transitions in pea leaves – Relationship between NADP/NADPH ratios and NADP-malate dehydrogenase activation state. *Plant Physiol.* **99**: 979–986.
- Fraser, P.D., and Bramley, P.M. (2004). The biosynthesis and nutritional uses of carotenoids. *Prog. Lipid Res.* **43**: 228–265.
- Fraser, P.D., Enfissi, E.M.A., Halket, J.M., Truesdale, M.R., Yu, D., Gerrish, C., and Bramley, P.M. (2007). Manipulation of phytoene levels in tomato fruit: effects on isoprenoids, plastids, and intermediary metabolism. *Plant Cell* **19**: 3194–3211.
- Fraser, P.D., Truesdale, M.R., Bird, C.R., Schuch, W., and Bramley, P.M. (1994). Carotenoid biosynthesis during tomato fruit-development. *Plant Physiol.* **105**: 405–413.
- Frommer, W.B., Mielchen, C., and Martin, T. (1994). Metabolic control of patatin promoters from potato in transgenic tobacco and tomato plants. *Plant Physiol. (Life Sci. Adv.)* **13**: 329–334.
- Fu, Y., Ballicora, M.A., Leykam, J.F., and Preiss, J. (1998). Mechanism of reductive activation of potato tuber ADP-glucose pyrophosphorylase. *J. Biol. Chem.* **273**: 25045–25052.
- Geigenberger, P., Fernie, A.R., Gibon, Y., Christ, M., and Stitt, M. (2000). Metabolic activity decreases as an adaptive response to low internal oxygen in growing potato tubers. *Biol. Chem.* **381**: 723–740.
- Geigenberger, P., Müller-Rober, B., and Stitt, M. (1999). Contribution of adenosine 5'-diphosphoglucose pyrophosphorylase to the control of starch synthesis is decreased by water stress in growing potato tubers. *Planta* **209**: 338–345.
- Geigenberger, P., Reimholz, R., Geiger, M., Merlo, L., Canale, V., and Stitt, M. (1997). Regulation of sucrose and starch metabolism in potato tubers in response to short-term water deficit. *Planta* **201**: 502–518.
- Geigenberger, P., Regierer, B., Nunes-Nesi, A., Leisse, A., Urbanczyk-Wochniak, E., Springer, F., van Dongen, J.T., Kossmann, J., and Fernie, A.R. (2005). Inhibition of de novo pyrimidine synthesis in growing potato tubers leads to a compensatory stimulation of the pyrimidine salvage pathway and a subsequent increase in biosynthetic performance. *Plant Cell* **17**: 2077–2088.
- Geigenberger, P., Stitt, M., and Fernie, A.R. (2004). Metabolic control analysis and regulation of the conversion of sucrose to starch in growing potato tubers. *Plant Cell Environ.* **27**: 655–673.
- Gibon, Y., Blaessing, O.E., Hannemann, J., Carillo, P., Höhne, M., Hendriks, J.H.M., Palacios, N., Cross, J., Selbig, J., and Stitt, M. (2004). A Robot-based platform to measure multiple enzyme activities

- in *Arabidopsis* using a set of cycling assays: Comparison of changes of enzyme activities and transcript levels during diurnal cycles and in prolonged darkness. *Plant Cell* **16**: 3304–3325.
- Gibon, Y., and Larher, F.** (1997). Cycling assay for nicotinamide adenine dinucleotides: NaCl precipitation and ethanol solubilization of the reduced tetrazolium. *Anal. Biochem.* **251**: 153–157.
- Giovannoni, J.J.** (2004). Genetic regulation of fruit development and ripening. *Plant Cell* **16** (suppl.): S170–S180.
- Giroux, M.J., and Hannah, L.C.** (1994). ADP-glucose pyrophosphorylase in shrunken-2 and brittle-2 mutants of maize. *Mol. Gen. Genet.* **243**: 400–408.
- Goodenough, P.W., Prosser, I.M., and Young, K.** (1985). NADP-linked malic enzyme and malate metabolism in aging tomato fruit. *Phytochemistry* **24**: 1157–1162.
- Hadfield, K.A., and Bennett, A.B.** (1998). Polygalacturonases: Many genes in search of a function. *Plant Physiol.* **117**: 337–343.
- Hirschberg, J.** (2001). Carotenoid biosynthesis in flowering plants. *Curr. Opin. Plant Biol.* **4**: 210–218.
- Huysamer, M., Greve, L.C., and Labavitch, J.M.** (1997). Cell wall metabolism in ripening fruit. 9. Synthesis of pectic and hemicellulosic cell wall polymers in the outer pericarp of mature green tomatoes (cv XMT-22). *Plant Physiol.* **114**: 1523–1531.
- Iglesias, A.A., Barry, G.F., Meyer, C., Bloksberg, L., Nakata, P.A., Greene, T., Laughlin, M.J., Okita, T.W., Kishore, G.M., and Preiss, J.** (1993). Expression of the potato tuber ADP-glucose pyrophosphorylase in *Escherichia coli*. *J. Biol. Chem.* **268**: 1081–1086.
- Isaacson, T., Kosma, D.K., Matas, A.J., Buda, G.J., He, Y., Yu, B., Pravitari, A., Batteas, J.D., Stark, R.E., Jenks, M.A., and Rose, J.K.** (2009). Cutin deficiency in the tomato fruit cuticle consistently affects resistance to microbial infection and biomechanical properties, but not transpirational water loss. *Plant J.* **60**: 363–377.
- Isaacson, T., Ohad, I., Beyer, P., and Hirschberg, J.** (2004). Analysis in vitro of the enzyme CRTISO establishes a poly-cis-carotenoid biosynthesis pathway in plants. *Plant Physiol.* **136**: 4246–4255.
- Jeffery, D., Smith, C., Goodenough, P., Prosser, I., and Grierson, D.** (1984). Ethylene-independent and ethylene-dependent biochemical changes in ripening tomatoes. *Plant Physiol.* **74**: 32–38.
- Jenner, H.L., Winning, B.M., Millar, A.H., Tomlinson, K.L., Leaver, C.J., and Hill, S.A.** (2001). NAD malic enzyme and the control of carbohydrate metabolism in potato tubers. *Plant Physiol.* **126**: 1139–1149.
- Kahlau, S., and Bock, R.** (2008). Plastid transcriptomics and translomics of tomato fruit development and chloroplast-to-chromoplast differentiation: Chromoplast gene expression largely serves the production of a single protein. *Plant Cell* **20**: 856–874.
- Kolbe, A., Tiessen, A., Schluepmann, H., Paul, M., Ulrich, S., and Geigenberger, P.** (2005). Trehalose 6-phosphate regulates starch synthesis via posttranslational redox activation of ADP-glucose pyrophosphorylase. *Proc. Natl. Acad. Sci. USA* **102**: 11118–11123.
- Lance, C., Hobson, G.E., Young, R.E., and Biale, J.B.** (1967). Metabolic processes in cytoplasmic particles of the avocado fruit. IX. The oxidation of pyruvate and malate during the climacteric cycle. *Plant Physiol.* **42**: 471–478.
- Laemmli, U.K.** (1970). Cleavage of structural proteins during the assembly of the head of bacteriophage T4. *Nature* **227**: 680–685.
- Lemaire-Chamley, M., Petit, J., Garcia, V., Just, D., Baldet, P., Germain, V., Fagard, M., Mouassite, M., Cheniclet, C., and Rothan, C.** (2005). Changes in transcriptional profiles are associated with early fruit tissue specialization in tomato. *Plant Physiol.* **139**: 750–769.
- Lewinsohn, E., et al.** (2001). Enhanced levels of the aroma and flavor compound S-linalool by metabolic engineering of the terpenoid pathway in tomato fruits. *Plant Physiol.* **127**: 1256–1265.
- Liu, X.J., Prat, S., Willmitzer, L., and Frommer, W.B.** (1990). Cis regulatory elements directing tuber-specific and sucrose-inducible expression of a chimeric class I patatin promoter/GUS-gene fusion. *Mol. Gen. Genet.* **223**: 401–406.
- Lunn, J.E., Feil, R., Hendriks, J.H.M., Gibon, Y., Morcuende, R., Osuna, D., Scheible, W.R., Carillo, P., Hajirezaei, M.R., and Stitt, M.** (2006). Sugar-induced increases in trehalose 6-phosphate are correlated with redox activation of ADP-glucose pyrophosphorylase and higher rates of starch synthesis in *Arabidopsis thaliana*. *Biochem. J.* **397**: 139–148.
- Maclachlan, G., and Brady, C.** (1994). Endo-1,4-beta-gluconase, xyloglucanase, and xyloglucan endo-transglycosylase activities versus potential substrates in ripening tomatoes. *Plant Physiol.* **105**: 965–974.
- Matas, A.J., Gapper, N.E., Chung, M.-Y., Giovannoni, J.J., and Rose, J.K.C.** (2009). Biology and genetic engineering of fruit maturation for enhanced quality and shelf-life. *Curr. Opin. Biotechnol.* **20**: 197–203.
- Michalska, J., Zauber, H., Buchanan, B.B., Cejudo, F.J., and Geigenberger, P.** (2009). NTRC links built-in thioredoxin to light and sucrose in regulating starch synthesis in chloroplasts and amyloplasts. *Proc. Natl. Acad. Sci. USA* **106**: 9908–9913.
- Moco, S., Capanoglu, E., Tikunov, Y., Bino, R.J., Boyacioglu, D., Hall, R.D., Vervoort, J., and De Vos, R.C.H.** (2007). Tissue specialization at the metabolite level is perceived during the development of tomato fruit. *J. Exp. Bot.* **58**: 4131–4146.
- Mounet, F., et al.** (2009). Gene and metabolite regulatory network analysis of early developing fruit tissues highlights new candidate genes for the control of tomato fruit composition and development. *Plant Physiol.* **149**: 1505–1528.
- Müller-Röber, B.T., Kossmann, J., Hannah, L.C., Willmitzer, L., and Sonnewald, U.** (1990). One of two different ADP-glucose pyrophosphorylase genes from potato responds strongly to elevated levels of sucrose. *Mol. Gen. Genet.* **224**: 136–146.
- Müller-Röber, B.T., Sonnewald, U., and Willmitzer, L.** (1992). Inhibition of the ADP-glucose pyrophosphorylase in transgenic potatoes leads to sugar-storing tubers and influences tuber formation and expression of tuber storage protein genes. *EMBO J.* **11**: 1229–1238.
- Murashige, T., and Skoog, F.** (1962). A revised medium for rapid growth and bioassays with tobacco tissue cultures. *Physiol. Plant.* **15**: 473–497.
- Nashilevitz, S., et al.** (2010). An orange ripening mutant links plastid NAD(P)H dehydrogenase complex activity to central and specialized metabolism during tomato fruit maturation. *Plant Cell* **22**: 1977–1997.
- Nielsen, T.H., Krapp, A., Roper-Schwarz, U., and Stitt, M.** (1998). The sugar-mediated regulation of genes encoding the small subunit of Rubisco and the regulatory subunit of ADP glucose pyrophosphorylase is modified by phosphate and nitrogen. *Plant Cell Environ.* **21**: 443–454.
- Niggeweg, R., Michael, A.J., and Martin, C.** (2004). Engineering plants with increased levels of the antioxidant chlorogenic acid. *Nat. Biotechnol.* **22**: 746–754.
- Nunes-Nesi, A., Carrari, F., Gibon, Y., Sulpice, R., Lytovchenko, A., Fisahn, J., Graham, J., Ratcliffe, R.G., Sweetlove, L.J., and Fernie, A.R.** (2007). Deficiency of mitochondrial fumarate activity in tomato plants impairs photosynthesis via an effect on stomatal function. *Plant J.* **50**: 1093–1106.
- Nunes-Nesi, A., Carrari, F., Lytovchenko, A., Smith, A.M.O., Loureiro, M.E., Ratcliffe, R.G., Sweetlove, L.J., and Fernie, A.R.** (2005). Enhanced photosynthetic performance and growth as a consequence of decreasing mitochondrial malate dehydrogenase activity in transgenic tomato plants. *Plant Physiol.* **137**: 611–622.
- Obidalla-Ali, H., Fernie, A.R., Lytovchenko, A., Kossmann, J., and Lloyd, J.R.** (2004). Inhibition of chloroplastic fructose 1,6-bisphosphatase

- in tomato fruits leads to decreased fruit size, but only small changes in carbohydrate metabolism. *Planta* **219**: 533–540.
- Pecker, I., Chamovitz, D., Linden, H., Sandmann, G., and Hirshberg, J.** (1992). A single polypeptide catalysing the conversion of phytoene to zeta-carotene is transcriptionally regulated during fruit ripening. *Proc. Natl. Acad. Sci. USA* **89**: 49624966.
- Regierer, B., Fernie, A.R., Springer, F., Perez-Melis, A., Leisse, A., Koehl, K., Willmitzer, L., Geigenberger, P., and Kossmann, J.** (2002). Starch content and yield increase as a result of altering adenylate pools in transgenic plants. *Nat. Biotechnol.* **20**: 1256–1260.
- Robinson, N.L., Hewitt, J.D., and Bennett, A.B.** (1988). Sink metabolism in tomato fruit : I. Developmental changes in carbohydrate metabolizing enzymes. *Plant Physiol.* **87**: 727–730.
- Rössner, U., Luedemann, A., Brust, D., Fiehn, O., Linke, T., Willmitzer, L., and Fernie, A.R.** (2001). Metabolic profiling allows comprehensive phenotyping of genetically or environmentally modified plant systems. *Plant Cell* **13**: 11–29.
- Roessner-Tunali, U., Hegemann, B., Lytovchenko, A., Carrari, F., Bruedigam, C., Granot, D., and Fernie, A.R.** (2003). Metabolic profiling of transgenic tomato plants overexpressing hexokinase reveals that the influence of hexose phosphorylation diminishes during fruit development. *Plant Physiol.* **133**: 84–99.
- Römer, S., Fraser, P.D., Kiano, J.W., Shipton, C.A., Misawa, N., Schuch, W., and Bramley, P.M.** (2000). Elevation of the provitamin A content of transgenic tomato plants. *Nat. Biotechnol.* **18**: 666–669.
- Rontein, D., Dieuaide-Noubhani, M., Dufourc, E.J., Raymond, P., and Rolin, D.** (2002). The metabolic architecture of plant cells. Stability of central metabolism and flexibility of anabolic pathways during the growth cycle of tomato cells. *J. Biol. Chem.* **277**: 43948–43960.
- Rose, J.K.C., Catalá, C., Gonzalez-Carranza, C.Z.H., and Roberts, J.A.** (2003). Plant cell wall disassembly. In *The Plant Cell Wall*, Vol. 8, J.K.C. Rose, ed (Oxford, UK: Blackwell Publishing), pp. 264–324.
- Rose, J.K.C., Hadfield, K.A., Labavitch, J.M., and Bennett, A.B.** (1998). Temporal sequence of cell wall disassembly in rapidly ripening melon fruit. *Plant Physiol.* **117**: 345–361.
- Rose, J.K.C., Lee, H.H., and Bennett, A.B.** (1997). Expression of a divergent expansin gene is fruit-specific and ripening-regulated. *Proc. Natl. Acad. Sci. USA* **94**: 5955–5960.
- Rose, J.K.C., Saladié, M., and Catalá, C.** (2004). The plot thickens: New perspectives of primary cell wall modification. *Curr. Opin. Plant Biol.* **7**: 296–301.
- Saladié, M., et al.** (2007). A reevaluation of the key factors that influence tomato fruit softening and integrity. *Plant Physiol.* **144**: 1012–1028.
- Saravanan, R.S., and Rose, J.K.C.** (2004). A critical evaluation of sample extraction techniques for enhanced proteomic analysis of recalcitrant plant tissues. *Proteomics* **4**: 2522–2532.
- Schaarschmidt, S., Roitsch, T., and Hause, B.** (2006). Arbuscular mycorrhiza induces gene expression of the apoplastic invertase LIN6 in tomato (*Lycopersicon esculentum*) roots. *J. Exp. Bot.* **57**: 4015–4023.
- Schaffer, A.A., and Petreikov, M.** (1997). Sucrose-to-starch metabolism in tomato fruit undergoing transient starch accumulation. *Plant Physiol.* **113**: 739–746.
- Schauer, N., Steinhauser, D., Strelkov, S., Schomburg, D., Allison, G., Moritz, T., Lundgren, K., Roessner-Tunali, U., Forbes, M.G., Willmitzer, L., Fernie, A.R., and Kopka, J.** (2005). GC-MS libraries for the rapid identification of metabolites in complex biological samples. *FEBS Lett.* **579**: 1332–1337.
- Scheibe, R.** (1991). Redox-modulation of chloroplast enzymes: A common principle for individual control. *Plant Physiol.* **96**: 1–3.
- Scheibe, R.** (2004). Malate valves to balance cellular energy supply. *Physiol. Plant.* **120**: 21–26.
- Schippers, J.H.M., Nunes-Nesi, A., Apetrei, R., Hille, J., Fernie, A.R., and Dijkwel, P.P.** (2008). The *Arabidopsis* onset of leaf death5 mutation of quinolinate synthase affects nicotinamide adenine dinucleotide biosynthesis and causes early ageing. *Plant Cell* **20**: 2909–2925.
- Seymour, G., Poole, M., Manning, K., and King, G.J.** (2008). Genetics and epigenetics of fruit development and ripening. *Curr. Opin. Plant Biol.* **11**: 58–63.
- Sienkiewicz-Porzucek, A., Nunes-Nesi, A., Sulpice, R., Lisec, J., Centeno, D.C., Carillo, P., Leisse, A., Urbanczyk-Wochniak, E., and Fernie, A.R.** (2008). Mild reductions in mitochondrial citrate synthase activity result in a compromised nitrate assimilation and reduced leaf pigmentation but have no effect on photosynthetic performance or growth. *Plant Physiol.* **147**: 115–127.
- Smidansky, E.D., Clancy, M., Meyer, F.D., Lanning, S.D., Blake, N.K., Talbert, L.E., and Giroux, M. J.** (2002). Enhanced ADP-glucose pyrophosphorylase activity in wheat endosperm increases seed yield. *Proc. Natl. Acad. Sci. USA* **99**: 1724–1729.
- Smith, A.M.** (2008). Prospects for increasing starch and sucrose yields for bioethanol production. *Plant J.* **54**: 546–558.
- Sowokinos, J.R.** (1981). Pyrophosphorylases in *Solanum tuberosum*: II. Catalytic properties and regulation of ADP-glucose and UDP-glucose pyrophosphorylase activities in potatoes. *Plant Physiol.* **68**: 924–929.
- Sowokinos, J.R., and Preiss, J.** (1982). Pyrophosphorylases in *Solanum tuberosum*: III. Purification, physical, and catalytic properties of ADP-glucose pyrophosphorylase in potatoes. *Plant Physiol.* **69**: 1459–1466.
- Stark, D.M., Timmerman, K.P., Barry, G.F., Preiss, J., and Kishore, G.M.** (1992). Regulation of the amount of starch in plant-tissues by ADP-glucose pyrophosphorylase. *Science* **258**: 287–292.
- Steinhauser, M.C., Steinhauser, D., Koehl, K., Carrari, F., Gibon, Y., Fernie, A.R., and Stitt, M.** (2010). Enzyme activity profiles during fruit development in tomato cultivars and *Solanum pennellii*. *Plant Physiol.* **153**: 80–98.
- Stitt, M., Lilley, R.M., Gerhardt, R., and Heldt, H.W.** (1989). Metabolite levels in specific cells and subcellular compartments of plant leaves. *Methods Enzymol.* **174**: 518–552.
- Sweetlove, L.J., Fait, A., Nunes-Nesi, A., Williams, T., and Fernie, A.R.** (2007). The mitochondrion: An integration point of cellular metabolism and signalling. *Crit. Rev. Plant Sci.* **26**: 17–43.
- Sweetlove, L.J., Muller-Rober, B., Willmitzer, L., and Hill, S.A.** (1999). The contribution of adenosine 5'-diphosphoglucose pyrophosphorylase to the control of starch synthesis in potato tubers. *Planta* **209**: 330–337.
- Sweetman, C., Deluc, L.G., Cramer, G.R., Ford, C.M., and Soole, K.L.** (2009). Regulation of malate metabolism in grape berry and other developing fruits. *Phytochemistry* **70**: 1329–1344.
- Tauberger, E., Fernie, A.R., Emmermann, M., Renz, A., Kossmann, J., Willmitzer, L., and Trethewey, R.N.** (2000). Antisense inhibition of plastidial phosphoglucomutase provides compelling evidence that potato tuber amyloplasts import carbon from the cytosol in the form of glucose-6-phosphate. *Plant J.* **23**: 43–53.
- Tieman, D., Taylor, M., Schauer, N., Fernie, A.R., and Klee, H.J.** (2006). Tomato aromatic amino acid decarboxylases participate in synthesis of flavor volatiles 2-phenylethanol and 2-phenylethanol and 2-phenylacetaldehyde. *Proc. Natl. Acad. USA* **103**: 8287–8292.
- Tiessen, A., Hendriks, J.H.M., Stitt, M., Branscheid, A., Gibon, Y., Farré, E.M., and Geigenberger, P.** (2002). Starch synthesis in potato tubers is regulated by post-translational redox modification of ADP-glucose pyrophosphorylase: A novel regulatory mechanism linking starch synthesis to the sucrose supply. *Plant Cell* **14**: 2191–2213.
- Tjaden, J., Möhlmann, T., Kampfenkel, K., Henrichs, G., and Neuhaus, H.E.** (1998). Altered plastidic ATP/ADP-transporter activity

- influences potato (*Solanum tuberosum* L.) tuber morphology, yield and composition of tuber starch. *Plant J.* **16**: 531–540.
- van der Merwe, M., Osorio, S., Moritz, T., Nunes-Nesi, A., and Fernie, A.R.** (2009). Decreased mitochondrial activities of malate dehydrogenase and fumarase in tomato lead to altered root growth and architecture via diverse mechanisms. *Plant Physiol.* **149**: 653–669.
- van der Merwe, M.J., Osorio, S., Araújo, W.L., Balbo, I., Nunes-Nesi, A., Maximova, E., Carrari, F., Bunik, V.I., Persson, S., and Fernie, A.R.** (2010). Tricarboxylic acid cycle activity regulates tomato root growth via effects on secondary cell wall production. *Plant Physiol.* **153**: 611–621.
- Vrebalov, J., Ruezinsky, D., Padmanabhan, V., White, R., Medrano, D., Drake, R., Schuch, W., and Giovannoni, J.** (2002). A MADS-box gene necessary for fruit ripening at the tomato ripening-inhibitor (*rin*) locus. *Science* **296**: 343–346.
- Vriezen, W.H., Feron, R., Maretto, F., Keijman, J., and Mariani, C.** (2008). Changes in tomato ovary transcriptome demonstrate complex hormonal regulation of fruit set. *New Phytol.* **177**: 60–76.
- Wang, F., Sanz, A., Brenner, M.L., and Smith, A.** (1993). Sucrose synthase, starch accumulation, and tomato fruit sink strength. *Plant Physiol.* **101**: 321–327.
- Wang, H., Schauer, N., Usadel, B., Frasse, P., Zouine, M., Hernould, M., Latché, A., Pech, J.-C., Fernie, A.R., and Bouzayen, M.** (2009). Regulatory features underlying pollination-dependent and -independent tomato fruit set revealed by transcript and primary metabolite profiling. *Plant Cell* **21**: 1428–1452.
- Wang, S., Liu, J., Feng, Y., Niu, X., Giovannoni, J., and Liu, Y.** (2008). Altered plastid levels and potential for improved fruit nutrient content by downregulation of the tomato DDB1-interacting protein CUL4. *Plant J.* **55**: 89–103.
- Woodrow, I.E., and Rowan, K.S.** (1979). Change of flux of orthophosphate between cellular compartments in ripening tomato fruits in relation to the climacteric rise in respiration. *Aust. J. Plant Physiol.* **6**: 39–46.
- Woitsch, S., and Römer, S.** (2003). Expression of xanthophyll biosynthetic genes during light-dependent chloroplast differentiation. *Plant Physiol.* **132**: 1508–1517.
- Zanor, M.I., et al.** (2009). RNA interference of LIN5 in tomato confirms its role in controlling Brix content, uncovers the influence of sugars on the levels of fruit hormones, and demonstrates the importance of sucrose cleavage for normal fruit development and fertility. *Plant Physiol.* **150**: 1204–1218.